


Ionization Constants of DL-2-Aminobutyric Acid and DL-Norvaline Under Hydrothermal Conditions by UV–Visible Spectroscopy

Daniel E. Nieto Roca¹ · Carmen M. Romero¹ · Peter R. Tremaine² 

Received: 19 July 2016 / Accepted: 26 November 2016 / Published online: 2 February 2017
© Springer Science+Business Media New York 2017

Abstract The first and second ionization constants for the amino acids DL-2-aminobutyric acid (DL-2-aminobutanoic acid) and DL-norvaline (DL-2-aminopentanoic acid) were determined under hydrothermal conditions, from 175 to 275 °C at 10 MPa, using thermally-stable colorimetric pH indicators (acridine, 4-nitrophenol and 2-naphthoic acid). The measurements were carried out by UV–visible spectroscopy using a high-temperature, high-pressure platinum flow cell with sapphire windows, which minimized the effects of thermal decomposition. The results were combined with literature values from titration calorimetry at 25–130 °C to yield an extended van't Hoff model for the temperature dependence of the ionization constants for the carboxylic acid and ammonium groups, $K_{a,COOH}$ and K_{a,NH_3^+} , over the entire temperature range. The experimental results for the second ionization constant K_{a,NH_3^+} at elevated temperatures are consistent with the predictions from the Yezdimer–Sedlbauer–Wood functional group additivity model, but for the first ionization constant $K_{a,COOH}$ are not. This suggests that the group contribution parameters for the standard partial molar heat capacity of the carboxylic acid group are in error, or that nearest neighbor interactions between the $-COOH$ and $-NH_3^+$ groups cause a breakdown in the functional group additivity relationship.

Keywords DL-2-aminobutyric acid · DL-norvaline · Ionization constants · Thermally-stable colorimetric pH indicator · Hydrothermal solutions · Group additivity relationship

Electronic supplementary material The online version of this article (doi:10.1007/s10953-017-0569-z) contains supplementary material, which is available to authorized users.

✉ Peter R. Tremaine
tremaine@uoguelph.ca

¹ Departamento de Química, Facultad de Ciencias, Universidad Nacional de Colombia, Calle 44 # 45-67 Bloque B9, Bogotá, Colombia

² Department of Chemistry, University of Guelph, Guelph, ON N1G 2W1, Canada

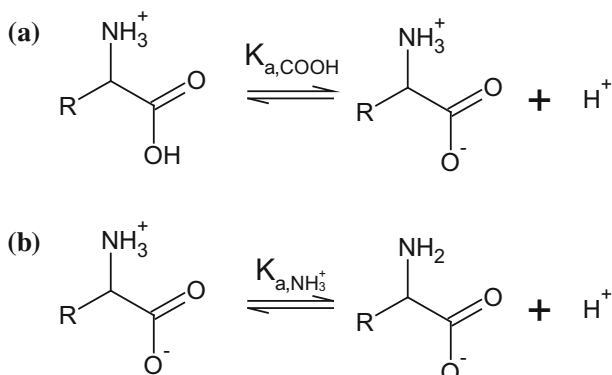
1 Introduction

The thermodynamic properties of aqueous amino acids [1, 2] under hydrothermal conditions are needed for modelling the behavior of complex aqueous systems such as those involved in biochemical and geochemical processes postulated for the origin of life at deep ocean vents [3, 4], for designing advanced carbon capture processes to reduce greenhouse gas emissions [5, 6], and for developing environmentally friendly chemical additives for pH control in industrial steam generators [2].

In aqueous solutions, amino acids exist as the protonated ion, H_2A^+ , the zwitterion, HA^\pm , and the deprotonated anion, A^- [1]. The equilibrium concentration of the non-zwitterionic form, HA^0 , is negligible at room temperature [7]. The ionization equilibria between these species are shown in Fig. 1. An in-depth analysis of the thermodynamic properties of amino acids would require an extensive database with the properties of all substances at these conditions, a task that is too extensive to be completed [1]. In the 1970s and 1980s, a number of functional group additivity models were developed which attempted to predict the values of standard thermodynamic properties for organic solutes under ambient conditions from the contributions of the different functional groups that form them [8, 9]. More recently, Amend and Helgeson [10] and Yezdimer et al. [11] have reported functional group additivity models that extend to hydrothermal conditions, based on the equations of state proposed by Tanger and Helgeson [12], Shock et al. [13] and Sedlbauer et al. [14], respectively. These models make use of a functional group specific to amino acids, $\text{^-OOC}-\overset{\text{|}}{\text{C}}-\text{NH}_3^+$ since the contributions of the individual NH_3^+ and COO^- groups failed to accurately describe the behavior of the zwitterion at hydrothermal conditions. However, since no experimental data were available for the anionic and cationic forms, $\text{HOOC}-\overset{\text{|}}{\text{C}}-\text{NH}_3^+$ and $\text{^-OOC}-\overset{\text{|}}{\text{C}}-\text{NH}_2$, no specific group parameters were proposed for these species. It becomes important, then, to compare the results from these predictions with actual experimental data to test the validity of the method.

The ionization constants of amino acids have been measured at near ambient conditions by a number of workers [6, 15–22]. The first ionization constants and enthalpies reported above 100 °C are values for six alkyl-amino acids at temperatures up to 125 °C, determined by Gillespie et al. [5, 6, 23, 24] and Wang et al. [5, 6, 23, 24], using isothermal flow

Fig. 1 The first and second ionization reactions for α -amino acids



mixing calorimetry. The first ionization constants for glycine, alanine and proline up to 250 °C, and the second ionization constant of glycine up to 125 °C, were measured in our laboratory by Clarke et al. [25] using a UV–visible spectroscopic flow cell with thermally stable colorimetric pH indicators to measure the equilibrium pH of buffer assemblages of the amino acid zwitterion with salts of the anion or cation. The advantages of this flow method over hydrothermal potentiometric titration methods in stirred vessels [26–28] are that the short residence time minimizes thermal decomposition, and that decomposition rates can be measured in situ by stopping the flow. The group additivity parameters for the amino acid zwitterion reported by Yezdimer et al. [11] were based on the standard partial molar heat capacities and volumes, C_p° and V° , of glycine and alanine reported by Hakin et al. [29], Clarke and Tremaine [30] and Clarke et al. [31] over the temperature range 25–250 °C. There are no experimental values of C_p° and V° for the cationic and anionic amino-acid salts, and we are aware of no other high-temperature ionization constant measurements for the amino acids in the literature.

Over the past several years, we have conducted a series of studies aimed at developing a database and functional group additivity relationships for amines, alkanolamines, carboxylic acids and amino acids and their salts under hydrothermal conditions up to the limits of their thermal stability [25, 30–32]. The purpose of the present study is to determine additional thermodynamic data for the first and second ionization constants of a series of 2-alkyl amino acids at temperatures approaching 300 °C, in order to the test accuracy of the functional group additivity model of Yezdimer et al. [11] under acidic and basic conditions up to the limits of its stated temperature range. This work extends our original measurements of the ionization constants of glycine and alanine (2-aminoethanoic acid and 2-aminopropanoic acid) [25] to longer *n*-alkyl chains, DL-2-aminobutyric acid and DL-norvaline (2-aminopentanoic acid). The studies were carried out at 10 MPa and temperatures as high as 275 °C using an improved UV–visible spectrophotometric flow cell system [33]. Particular care was given to the selection and cross-calibration of colorimetric pH indicators required to determine the second ionization constants of the amino acids over the entire temperature range, as these were not included in the study by Clarke et al. [25].

2 Experimental

2.1 Chemicals

Solutions were prepared by mass from dried solids or carefully standardized solutions using distilled, deionized and degassed water (resistivity = 18 MΩ·cm). Concentrated solutions of NaOH (mass fraction 50.1%, Fisher Scientific ACS) and HCl (mass fraction 35%, Fisher Scientific ACS) were used to prepare stock solutions. The NaOH solutions were standardized by triplicate titration using potassium hydrogen phthalate (Fischer Scientific, 100.05%), that had been dried at 110 °C for 2 h prior to use. The HCl solutions were standardized by titration with the previously standardized NaOH. All NaOH solutions were stored in tightly sealed Nalgene bottles, and transferred quickly to avoid contamination by atmospheric CO₂.

DL-2-aminobutyric acid (“Assay 99%”, Aldrich) and DL-norvaline (Sigma Grade, Sigma) were stored in a desiccator under vacuum for at least 48 h prior to their use. Acridine (“Assay 97%”, Sigma–Aldrich), 2-naphthoic acid (“Assay 98%”, Aldrich) and 4-nitrophenol (“Assay ≥ 99%”, Sigma–Aldrich) were used as received.

Acridine was used as indicator to determine the ionization constant of the carboxylate group, while either 2-naphthoic acid or 4-nitrophenol, depending on the temperature, was used for the ionization of the amino group. Stock indicator solutions were prepared fresh each night, to be used the next day. To ensure that the indicators dissolved completely, they were combined with a known amount of either dilute HCl, to form acridinium chloride, or dilute NaOH, to form the sodium salts of 2-naphthoic acid and 4-nitrophenol. The basic and acid extremes for each indicator were prepared as follows: 3 mL aliquots of the stock indicator solutions were transferred into two 30 mL Nalgene bottles. An excess of HCl was added to one of the bottles, and an excess of NaOH to the other, ensuring the presence of only the acid or the basic species of the indicator, respectively. The solutions were then diluted to 30 mL with water. At each step, the masses of the solutions and added water were recorded. The solutions were stirred overnight in sealed Nalgene bottles, which were covered with aluminum foil to avoid contact with air and light.

Buffer solutions were prepared by adding a known mass of HCl or NaOH solution to aliquots of the stock amino acid solution. Approximately 3 mL of dissolved indicator solution were added to each buffer by mass so that the concentration of the indicator was close to the ones in the basic and acid extremes. The amount of HCl or NaOH used to dissolve the indicator was taken into account in the calculations to determine the buffer ratio in each solution. Finally, the ionic strength of the solutions was adjusted with additions by mass of crystalline sodium chloride (Fisher Scientific, ACS certified).

2.2 Apparatus

The equilibrium constants were measured in a high-temperature, high-pressure spectroscopic flow system, similar to that described by Trevani et al. [34], with the modifications introduced by Bulemela and Tremaine [33]. The system consisted of a low volume platinum cell with sapphire windows, contained in a titanium casing. The cell was secured in a brass oven containing two Chromalux CIR-20203 cartridge heaters. To preheat the solution, a coil made of small diameter platinum tubing was placed in a groove cut in the body of the brass oven. The cell was located in the sample compartment of a Cary 50 UV–visible spectrometer, capable of fast acquisition of digitalized spectral data. The total volume of the system is 0.65 cm³ (cell, 0.35 cm³; preheater, 0.30 cm³).

Solutions were degassed in syringes by suction and then loaded into an injection loop. There was a constant flow of water, which was pumped into the system by a high-pressure liquid chromatography pump, going through the preheater before arriving at the platinum cell. By changing the position of a six-way valve, water pushed the solution from the injection loop into the system. Teflon or gold washers were used to assure that the solutions will only be in contact with gold, Teflon, sapphire or platinum when under hydrothermal conditions. The pressure of the system was maintained at (10 ± 0.2) MPa by the use of a high-pressure adjustable Back Pressure Regulator (Upchurch Scientific). The system pressure was measured with a Gilson 805 manometric module. The temperature was maintained to ± 0.1 °C by an Omega CN 7600 temperature controller, with a Chromega–Alomega thermocouple located near the sample chamber of the cell.

2.3 Methods

Deionized water was injected into the cell at a constant volumetric flow of 1 cm³·min⁻¹ and a constant pressure of 10 MPa. Samples of each solution (approximately 15 mL) were introduced by means of a high-pressure liquid chromatography injection loop. The spectra

were not collected until the absorption band intensity was stable, to ensure that the water in the cell had been completely replaced by the injected sample. Five spectra of each solution were recorded and averaged to minimize noise. The wavelength range was 260–500 nm, except for samples containing 4-nitrophenol where the range was 260–550 nm. To account for the slight absorption of the amino acids in the wavelength range of work, the spectra of the same buffer solutions without the indicator were used as baseline for each measurement. The temperature ranges studied were from 150 to 275 °C for the carboxylate ionization constants and from 175 to 275 °C for the amino ionization constants, both with 25 °C steps.

Colorimetric indicators consist of species that exist in equilibrium between an acid form and its conjugate base, in which each form has a different UV–visible spectrum. The relative concentration of each form is dependent on the pH of the solution so that, if both are present, the spectrum of the mixture is a linear combination of the spectra of the two species. If the spectra for the acid form of the indicator and its conjugate base are determined independently, then the ratio between the two species in the mixture can be found from its UV–visible spectrum, and the pH of the solution can be calculated.

The ionization constants for both the carboxylic acid group ($K_{a,COOH}$) and the aminium (K_{a,NH_3^+}) groups of DL-2-aminobutyric acid and DL-norvaline were measured following the procedure of Clarke et al. [25]. The choice of indicator for each run was guided by extrapolations of room temperature data using the van't Hoff equation. Plots for DL-2-aminobutyric acid are shown in Fig. 2 as an example. The area of overlap between ($pK_{HI_{ind}^+} \pm 1$) and the predicted pK for the reaction corresponds to the expected practical limits for meaningful measurements. Figure 2a shows the predicted indicator range of acridine (Minubayeva et al. [35]) with the values of $pK_{a,COOH}$ for DL-2-aminobutyric acid predicted from low temperature data (Wang et al. [24]). Based on these results, acridine was chosen as the indicator for the measurements of the ionization constants of the carboxylate groups of both amino acids in a range from 150 to 275 °C. For the ionization of the amino group, two different UV–visible indicators were used. 4-Nitrophenol was used for the measurements at 175 and 200 °C, whereas 2-naphthoic acid was used for temperatures above 200 °C. The predicted ranges for 2-naphthoic acid and 4-nitrophenol are shown in Fig. 2b, c, respectively, with extrapolated values of pK_{a,NH_3^+} for DL-2-aminobutyric acid (Gillespie et al. [23]). The need of two different indicators was due to the fact that neither of them could be used over the entire temperature range of the study because the effective indicator range of 2-naphthoic acid is too small [28] and thermal decomposition of 4-nitrophenol occurs above 200 °C [36]. Since the effective range for both indicators overlap close to 200 °C, separate measurements for the second ionization constant of DL-2-aminobutyric acid at this temperature were made with each as a means to compare the results obtained.

Stopped flow experiments were conducted to account for possible decomposition of the substances in the cell. In these, the flow was stopped after the cell was filled with solution, allowing prolonged exposure to the high pressure and temperature conditions. During this time, UV–visible spectra were taken every 2 min. These results showed that, even though decomposition occurred, the short residence time of the sample in the cell during the measurements (less than 1 min) resulted in the decomposition being negligible.

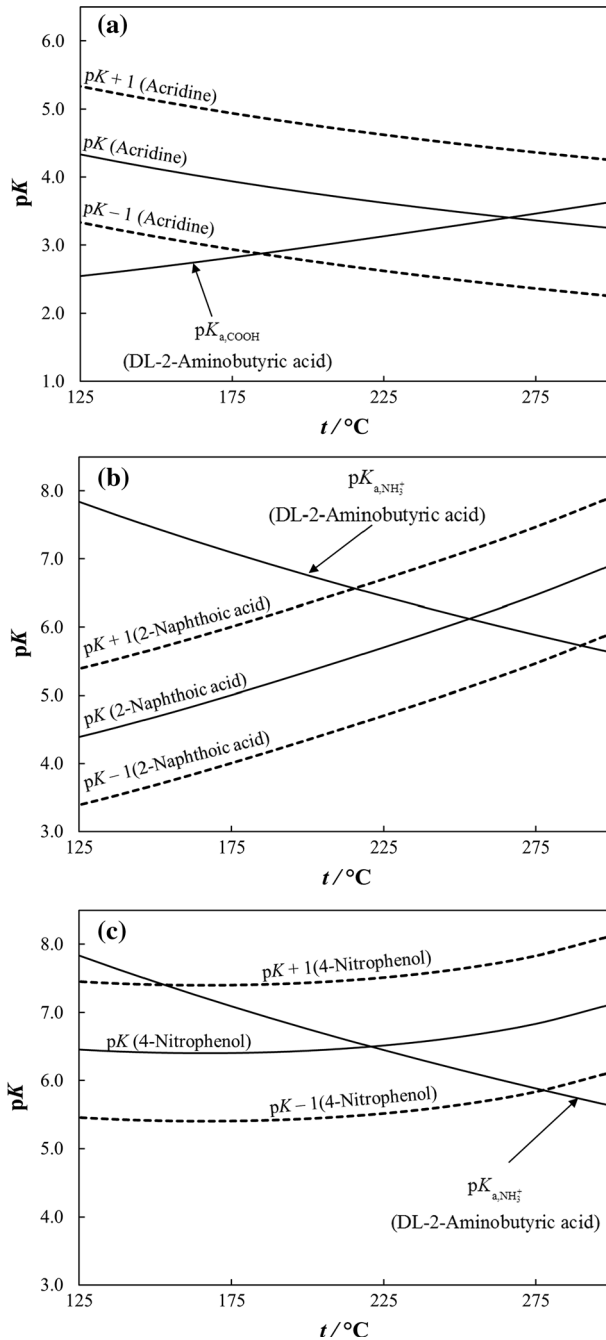
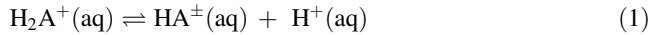


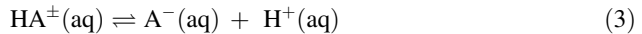
Fig. 2 Predicted indicator ranges, defined as $\text{p}K_{\text{HInd}^+} \pm 1 \log_{10}$ unit, and the temperature dependence of the ionization constants of DL-2-aminobutyric acid, as estimated from room temperature thermodynamic data: **a** acridine (Minubayeva et al. [35]); **b** 2-naphthoic acid (Xiang and Johnston [28]); **c** 4-nitrophenol (Ehlerova et al. [36])

2.4 Spectroscopic and Equilibrium Constant Analysis

In the analysis that follows, the equilibria used to represent the dissociation of protonated and zwitterionic forms of the amino acids are



$$K_{\text{a,COOH}} = \frac{m_{\text{H}^+} m_{\text{HA}^\pm} \gamma_{\text{H}^+} \gamma_{\text{HA}^\pm}}{m_{\text{H}_2\text{A}^+} \gamma_{\text{H}_2\text{A}^+}} \quad (2)$$



$$K_{\text{a,NH}_3^+} = \frac{m_{\text{A}^-} m_{\text{H}^+} \gamma_{\text{A}^-} \gamma_{\text{H}^+}}{m_{\text{HA}^\pm} \gamma_{\text{HA}^\pm}} \quad (4)$$

where m_{H^+} , m_{HA^\pm} , $m_{\text{H}_2\text{A}^+}$ and m_{A^-} are the molalities of the hydrogen ion and the amino acid in its zwitterionic, protonated and anionic forms, respectively. $K_{\text{a,COOH}}$ and $K_{\text{a,NH}_3^+}$ are the thermodynamic equilibrium constants for reactions (1) and (3), respectively. In this study the equilibrium constant for the reaction

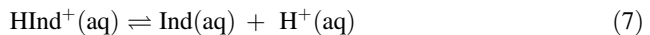


$$K_{\text{HA}^0} = \frac{m_{\text{HA}^\pm} \gamma_{\text{HA}^\pm}}{m_{\text{HA}^0} \gamma_{\text{HA}^0}} \quad (6)$$

was assumed to be very large at all temperatures, so the concentration of amino acid in the non-zwitterionic form is negligible.

Literature values for the temperature dependent ionization constants of acridine reported by Ryan et al. [26] and Minubayeva et al. [35], 2-naphthoic acid from Xiang and Johnston [28] and 4-nitrophenol from Ehlerova et al. [36] were used to calculate the dissociation constants of the amino acids in this study.

The acid dissociation of acridinium ion to acridine can be represented by



$$K_{\text{HInd}^+} = \frac{m_{\text{Ind}} m_{\text{H}^+} \gamma_{\text{Ind}} \gamma_{\text{H}^+}}{m_{\text{HInd}^+} \gamma_{\text{HInd}^+}} \quad (8)$$

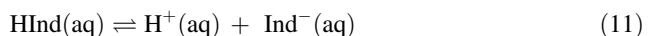
which can be determined from one of the following expressions:

$$\log_{10} K_{\text{HAc}^+} = -0.78794 - \frac{1411.767}{T} \quad (9)$$

from Minubayeva et al. [35], or

$$\ln K_{\text{HAc}^+} = -12.43 - 3663.04 \left(\frac{1}{T} - \frac{1}{T_r} \right) - \frac{15874.31}{T} \left(\frac{1}{\varepsilon} - \frac{1}{\varepsilon_r} \right), \quad (10)$$

from Ryan et al. [26]. The acid dissociation for 2-naphthoic acid and 4-nitrophenol can be represented by



$$K_{\text{HInd}} = \frac{m_{\text{Ind}^-} m_{\text{H}^+} \gamma_{\text{Ind}^-} \gamma_{\text{H}^+}}{m_{\text{HInd}} \gamma_{\text{HInd}}} \tag{12}$$

where HInd (aq) is the acidic form of the indicator. The expression for the dissociation constant for 2-naphthoic acid from Xiang and Johnston [28] is

$$\log_{10} K_{2\text{-NaphCOOH}} = -13.553 + \frac{7.824 \times 10^3}{T} - \frac{1.704 \times 10^6}{T^2} + \frac{6.318 \times 10^4}{T^3} + k \log \rho_w \tag{13}$$

with

$$k = -19.193 + \frac{1.974 \times 10^4}{T} - \frac{13.336 \times 10^4}{T^2} \tag{14}$$

Likewise, the expression for 4-nitrophenol from Ehlerova et al. [36] is

$$\begin{aligned} \ln K_{4\text{-NitrophOH}} &= \log_{10} K_{4\text{-NitrophOH}}(\ln 10) \\ &= -110.51 + \frac{6400.6}{T} + \left(14.899 - \frac{1307.4}{T} \right) \ln \rho_w \end{aligned} \tag{15}$$

In these equations, T is the temperature in Kelvin and ρ_w is the density of water in $\text{g}\cdot\text{cm}^{-3}$, which was calculated from the NIST database. The calculated values for $\log_{10} K$ for the indicators, based on the expressions given, are reported in Table 1. The molality of H^+ can be determined by rearranging Eqs. 8 and 12. Equation 8 then becomes

Table 1 Calculated values of $\text{p}K$ for the indicators used

$\frac{t}{^\circ\text{C}}$	$\text{p}K_{\text{HAc}^+}$ (acridine)		$\text{p}K_{2\text{-NaphCOOH}}$ (2-naphthoic Acid)	$\text{p}K_{4\text{-NitrophOH}}$ (4-nitrophenol)
	Equation 9 ^a	Equation 10 ^b	Equation 13 ^c	Equation 15 ^d
25	5.523	5.397	3.860	7.122
50	5.157	5.019	3.923	6.869
75	4.843	4.697	3.974	6.680
100	4.571	4.423	4.145	6.545
125	4.334	4.187	4.391	6.457
150	4.124	3.983	4.684	6.411
175	3.938	3.807	5.006	6.406
200	3.772	3.655	5.348	6.440
225	3.622	3.525	5.705	6.517
250	3.487	3.417	6.076	6.644
275	3.363	3.332	6.471	6.836

^a From Minubayeva et al. [35]

^b From Ryan et al. [26]

^c From Xiang and Johnston [28]

^d From Ehlerova et al. [36]

$$m_{\text{H}^+} = K_{\text{HInd}^+} \left(\frac{m_{\text{HInd}^+}}{m_{\text{Ind}}} \right) \left(\frac{\gamma_{\text{HInd}^+}}{\gamma_{\text{Ind}} \gamma_{\text{H}^+}} \right) \quad (16)$$

and Eq. 12 becomes

$$m_{\text{H}^+} = K_{\text{HInd}} \left(\frac{m_{\text{HInd}}}{m_{\text{Ind}^-}} \right) \left(\frac{\gamma_{\text{HInd}}}{\gamma_{\text{Ind}^-} \gamma_{\text{H}^+}} \right) \quad (17)$$

Substituting Eq. 16 into Eq. 2 gives an expression for the first ionization constant for the amino acid

$$K_{\text{a,COOH}} = K_{\text{HInd}^+} \left(\frac{m_{\text{HInd}^+}}{m_{\text{Ind}}} \right) \left(\frac{m_{\text{HA}^\pm}}{m_{\text{H}_2\text{A}^+}} \right) \left(\frac{\gamma_{\text{HInd}^+} \gamma_{\text{HA}^\pm}}{\gamma_{\text{Ind}} \gamma_{\text{H}_2\text{A}^+}} \right) \quad (18)$$

In an analogous way, substituting Eq. 17 in Eq. 4 yields the expression for the second ionization constant,

$$K_{\text{a,NH}_3^+} = K_{\text{HInd}} \left(\frac{m_{\text{A}^-}}{m_{\text{HA}^\pm}} \right) \left(\frac{m_{\text{HInd}}}{m_{\text{Ind}^-}} \right) \left(\frac{\gamma_{\text{HInd}} \gamma_{\text{A}^-}}{\gamma_{\text{Ind}^-} \gamma_{\text{HA}^\pm}} \right) \quad (19)$$

The activity coefficients for the neutral species, including HA^\pm , were assumed to be unity over all the concentration and temperature ranges. Ionic activity coefficients were assumed to depend solely on charge and ionic strength [37], so that in Eq. 18 $\gamma_{\text{HInd}^+}/\gamma_{\text{H}_2\text{A}^+} = 1$ and in Eq. 19 $\gamma_{\text{A}^-}/\gamma_{\text{Ind}^-} = 1$. These approximations simplify the expressions so that

$$K_{\text{a,COOH}} = K_{\text{HInd}^+} \left(\frac{m_{\text{HA}^\pm}}{m_{\text{H}_2\text{A}^+}} \right) \left(\frac{m_{\text{HInd}^+}}{m_{\text{Ind}}} \right) \quad (20)$$

$$K_{\text{a,NH}_3^+} = K_{\text{HInd}} \left(\frac{m_{\text{A}^-}}{m_{\text{HA}^\pm}} \right) \left(\frac{m_{\text{HInd}}}{m_{\text{Ind}^-}} \right) \quad (21)$$

In these two equations, the first molality ratio is the buffer ratio that can be calculated from the initial composition of the solutions. The second ratio is the indicator ratio that can be determined from the UV–visible spectra, in which the absorbance is treated as a linear combination of the spectra of both forms of the indicator. With this, and by using Beer's law, the following expression is obtained

$$A(\lambda) = [\varepsilon_{\text{HInd}^+}(\lambda) b m_{\text{HInd}^+}^* + \varepsilon_{\text{Ind}}(\lambda) b m_{\text{Ind}}^*] \rho_{\text{solution}} \quad (22)$$

where $A(\lambda)$ is the absorbance at each wavelength, b is the path length, and m_i^* is the concentration of species i , expressed for convenience as specific molality, $\text{mol} \cdot \text{kg}_{(\text{solution})}^{-1}$, instead of the usual $\text{mol} \cdot \text{kg}_{(\text{solvent})}^{-1}$. The relationship between specific molality and molarity is $m^* = C/\rho$. In this equation and the analysis that follows, “HInd” is used to designate the protonated form of the indicator and “Ind” to designate the deprotonated form. The terms $\varepsilon_{\text{HInd}}(\lambda)$ and $\varepsilon_{\text{Ind}}(\lambda)$ are the absorptivities for the indicator in its acid form and its conjugated base. These were determined from independent experiments with indicator solutions with excess of HCl and NaOH, respectively:

$$\varepsilon_{\text{HInd}}(\lambda) = \frac{A_{\text{acid}}(\lambda)}{b m_{\text{acid}}^* \rho_{\text{acid}}} \quad (23)$$

$$\varepsilon_{\text{Ind}}(\lambda) = \frac{A_{\text{base}}(\lambda)}{bm_{\text{base}}^* \rho_{\text{base}}} \quad (24)$$

Here, m_{acid}^* and m_{base}^* are the indicator concentrations in the acid (excess HCl) and basic (excess NaOH) extrema solutions, respectively. Substituting these two expressions into Eq. 22 and rearranging gives

$$\frac{A(\lambda)}{b\rho_{\text{solution}}} = \frac{A_{\text{acid}}(\lambda)}{bm_{\text{acid}}^* \rho_{\text{acid}}} \left(m_{\text{HInd}} + \frac{\rho_{\text{acid}} A_{\text{base}}(\lambda)}{\rho_{\text{base}} A_{\text{acid}}(\lambda)} D m_{\text{Ind}}^* \right) \quad (25)$$

where $D = m_{\text{acid}}^*/m_{\text{base}}^* \rho_{\text{acid}}$ is the density of the acid extremum solution and ρ_{base} is the density of the basic extremum solution. This expression was simplified even more by assuming the densities of the solutions were approximately equal, taking into account that the solutions were highly diluted. This gives

$$A(\lambda) = A_{\text{acid}}(\lambda) \frac{m_{\text{HInd}}^*}{m_{\text{acid}}^*} + A_{\text{base}}(\lambda) D \frac{m_{\text{Ind}}^*}{m_{\text{acid}}^*} \quad (26)$$

$$A(\lambda) = A_{\text{acid}}(\lambda)k + A_{\text{base}}(\lambda)Dl \quad (27)$$

The constants k and l were determined by least-squares regression of the experimental spectra, and from them the indicator ratio was calculated:

$$\frac{k}{l} = \frac{m_{\text{HInd}}^*}{m_{\text{Ind}}^*} = \frac{m_{\text{HInd}}}{m_{\text{Ind}}} \quad (28)$$

The ionization constants were calculated from the indicator ratio and with Eqs. 20 and 21, using the values for the ionization constants for the appropriate indicator.

3 Results

3.1 Ionization Constant for the Carboxylic Acid Group, $K_{\text{a,COOH}}$

Figure 3 shows the spectra for acridine in aqueous HCl (the acid extreme), in aqueous NaOH (the basic extreme) and in a series of DL-2-aminobutyric acid buffers. All spectra were normalized to the concentration of indicator in the acid extreme to account for the small differences in indicator concentration. As expected, the spectra for the buffer solutions fall between the spectra for the basic and the acid extremes, A_{acid} and A_{base} . Equation 27 was then fitted for each of the buffer spectra in the range between 300 and 475 nm, which is the range that showed the most statistically significant agreement between the fitted and the experimental spectra. This corresponds to the greatest difference in the absorption spectra of the two forms of the indicator. The results from the regression were used in Eq. 28 to obtain the indicator ratio, k/l . The solution compositions and the fitted values for parameters k and l for each buffer are listed in Tables 2 and 3 for DL-2-aminobutyric acid and DL-norvaline, respectively. Best results were obtained for buffer ratios $m_{\text{HA}\pm}/m_{\text{H}_2\text{A}^+} \geq 1.0$. Tables 4 and 5 list the ionization constants, $K_{\text{a,COOH}}$, for DL-2-aminobutyric acid and DL-norvaline calculated from Eq. 20, using the values from Minubayeva et al. [35], Eq. 9, and Ryan et al. [26], Eq. 10, to determine K_{HAc^+} . Figure 4 shows the values for $\text{p}K_{\text{a,COOH}}$ for 4(a) DL-2-aminobutyric acid and 4(b) DL-norvaline obtained in this study, along with results at lower temperatures from the literature

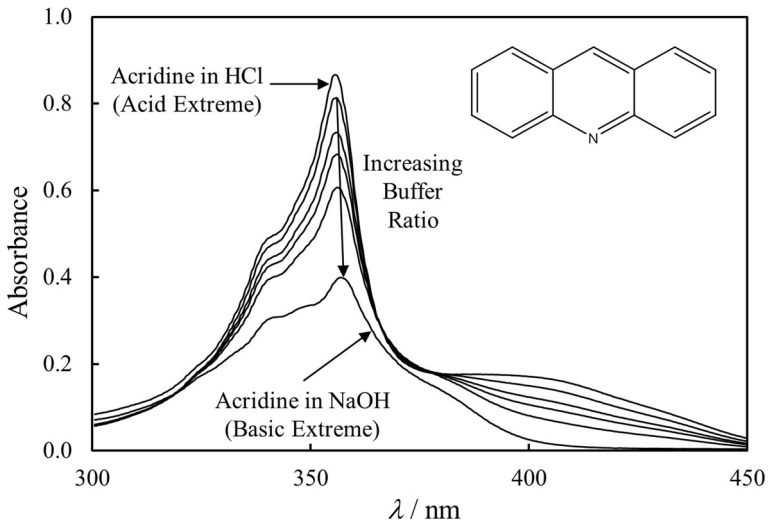


Fig. 3 UV–visible spectra of acridine at 225 °C in HCl (acid extreme), NaOH (basic extreme) and DL-2-aminobutyric acid buffers. The buffer ratio HA^\pm/H_2A^+ increases in the direction of the arrow

Table 2 The fitting parameters k and l for $K_{a,COOH}$ of DL-2-aminobutyric acid

t °C	Concentration ratio, D^a	Buffer ratio ^b	Acridine indicator ratio ^c	k	l
200.0 ± 0.1	0.9752	15.35	0.5842	0.4086 ± 0.0033	0.6995 ± 0.0059
	0.9752	10.38	0.8499	0.4988 ± 0.0034	0.5869 ± 0.0061
	0.9752	5.180	1.778	0.6796 ± 0.0034	0.3822 ± 0.0060
	0.9752	3.078	2.967	0.7749 ± 0.0037	0.2612 ± 0.0065
225.0 ± 0.1	0.9974	16.49	0.3820	0.3008 ± 0.0054	0.7875 ± 0.0094
	0.9974	10.81	0.5621	0.3859 ± 0.0052	0.6865 ± 0.0091
	0.9974	5.271	1.136	0.5615 ± 0.0050	0.4941 ± 0.0086
	0.9974	3.127	1.955	0.6858 ± 0.0051	0.3508 ± 0.0088
250.0 ± 0.1	1.001	14.38	0.3024	0.2759 ± 0.0068	0.9125 ± 0.0121
	1.001	9.921	0.4001	0.3319 ± 0.0066	0.8295 ± 0.0116
	1.001	5.021	0.8085	0.5128 ± 0.0072	0.6342 ± 0.0128
	1.001	3.012	1.381	0.6502 ± 0.0076	0.4709 ± 0.0135
275.0 ± 0.1	1.001	14.10	0.1740	0.1689 ± 0.0015	0.9710 ± 0.0026
	1.001	9.822	0.2572	0.2334 ± 0.0041	0.9077 ± 0.0070
	1.001	4.982	0.5097	0.3851 ± 0.0051	0.7556 ± 0.0088
	1.001	3.000	0.8222	0.5046 ± 0.0055	0.6138 ± 0.0094
	1.001	1.002	2.483	0.7764 ± 0.0057	0.3128 ± 0.0098

^a Defined as m_{acid}^*/m_{base}^*

^b Defined as $m_{HA^\pm}/m_{H_2A^+}$

^c Defined as m_{HInd}/m_{Ind}

Table 3 The fitting parameters k and l for $K_{a,COOH}$ of DL-norvaline

t °C	Concentration ratio, D^a	Buffer ratio ^b	Acridine indicator ratio ^c	k	l
175.0 ± 0.1	0.9903	15.293	0.8737	0.4905 ± 0.0030	0.5614 ± 0.0054
	0.9903	12.191	1.0662	0.5344 ± 0.0029	0.5012 ± 0.0053
	0.9903	10.122	1.3239	0.5909 ± 0.0029	0.4463 ± 0.0052
	0.9903	5.044	2.7497	0.7402 ± 0.0034	0.2692 ± 0.0062
200.0 ± 0.1	1.001	15.549	0.5535	0.3726 ± 0.0037	0.6731 ± 0.0064
	1.001	12.431	0.6973	0.4270 ± 0.0037	0.6123 ± 0.0065
	1.001	10.269	0.8430	0.4704 ± 0.0038	0.5580 ± 0.0066
	1.001	5.084	1.7685	0.6481 ± 0.0036	0.3665 ± 0.0063
225.0 ± 0.1	1.001	3.041	2.8798	0.7491 ± 0.0029	0.2601 ± 0.0051
	1.001	15.107	0.3534	0.2882 ± 0.0032	0.8154 ± 0.0058
	1.001	12.102	0.4373	0.3316 ± 0.0034	0.7583 ± 0.0060
	1.001	10.046	0.5295	0.3741 ± 0.0036	0.7065 ± 0.0064
250.0 ± 0.1	1.001	5.024	1.0527	0.5435 ± 0.0036	0.5163 ± 0.0064
	1.001	3.009	1.8291	0.6678 ± 0.0043	0.3651 ± 0.0077
	0.9760	15.570	0.2257	0.2121 ± 0.0034	0.9400 ± 0.0061
	0.9760	12.405	0.2723	0.2454 ± 0.0033	0.9013 ± 0.0061
275.0 ± 0.1	0.9760	10.249	0.3248	0.2788 ± 0.0032	0.8585 ± 0.0059
	0.9760	5.095	0.6492	0.4358 ± 0.0036	0.6714 ± 0.0066
	0.9760	3.039	1.0757	0.5605 ± 0.0033	0.5211 ± 0.0060
	1.000	19.628	0.1176	0.1223 ± 0.0023	1.0398 ± 0.0037
275.0 ± 0.1	1.000	15.005	0.1494	0.1511 ± 0.0023	1.0114 ± 0.0043
	1.000	12.011	0.1951	0.1893 ± 0.0033	0.9700 ± 0.0061
	1.000	5.555	0.4063	0.3285 ± 0.0040	0.8085 ± 0.0076
	1.000	3.255	0.6867	0.4558 ± 0.0040	0.6637 ± 0.0074

^a Defined as m_{acid}^*/m_{base}^*

^b Defined as $m_{HA^\pm}/m_{H_2A^+}$

^c Defined as m_{HInd}/m_{Ind}

[16–19, 24, 38]. The statistical uncertainty for each experimental value was calculated from the standard deviations of k and l . Values obtained for the ionization constant of both amino acids at 150 °C and of DL-2-aminobutyric acid at 175 °C were found to lie outside the effective indicator range, an expected result based on the extrapolation from room temperature data.

A clear difference was observed between the values obtained from each of the two expressions for K_{HAcr^+} . Higher values were always obtained from the indicator parameters reported by Minubayeva et al. [35] (Eq. 9), than those of Ryan et al. [26] (Eq. 10), with higher discrepancies at lower temperatures. The results show similar trends for both amino acids, where the value of $pK_{a,COOH}$ passes through a minimum at approximately 50 °C. The difference in $pK_{a,COOH}$ between the two amino acids ranges from 0.0145 at 200.0 °C, to 0.0899 at 250.0 °C.

Table 4 Experimental values of the first ionization constant of DL-2-aminobutyric acid, $pK_{a,COOH}$

t °C	$I \times 10^2$ mol·kg ⁻¹	Buffer ratio	Acridine indicator ratio	$pK_{a,COOH}$ results with Eq. 9 ^a		$pK_{a,COOH}$ results with Eq. 10 ^b	
				Experimental ^c	Average ^d	Experimental ^c	Average ^d
200.0 ± 0.1	5.0335	15.35	0.5842	2.819 ± 0.007	2.816 ± 0.007	2.702 ± 0.007	2.699 ± 0.007
	4.9961	10.38	0.8499	2.826 ± 0.008		2.709 ± 0.008	
	5.0331	5.180	1.778	2.807 ± 0.009		2.691 ± 0.009	
	5.0279	3.078	2.966	2.811 ± 0.013		2.694 ± 0.013	
	5.0335	16.49	0.3820	2.823 ± 0.013	2.835 ± 0.008	2.726 ± 0.013	2.738 ± 0.008
225.0 ± 0.1	4.9961	10.81	0.5621	2.838 ± 0.012		2.741 ± 0.012	
	5.0331	5.271	1.136	2.844 ± 0.011		2.748 ± 0.011	
	5.0279	3.127	1.955	2.836 ± 0.0142		2.739 ± 0.014	
	5.0418	14.38	0.3024	2.848 ± 0.016	2.870 ± 0.015	2.779 ± 0.016	2.801 ± 0.015
	5.0095	9.921	0.4001	2.888 ± 0.015		2.818 ± 0.015	
250.0 ± 0.1	5.0371	5.021	0.8085	2.878 ± 0.015		2.808 ± 0.015	
	5.0329	3.012	1.381	2.868 ± 0.017		2.798 ± 0.018	
	5.0335	14.10	0.1740	2.974 ± 0.005	2.966 ± 0.006	2.942 ± 0.005	2.934 ± 0.006
	4.9961	9.822	0.2572	2.961 ± 0.011		2.929 ± 0.011	
	5.0331	4.982	0.5097	2.959 ± 0.011		2.927 ± 0.011	
275.0 ± 0.1	5.0279	3.000	0.8222	2.971 ± 0.011		2.939 ± 0.011	
	5.0301	1.002	2.483	2.968 ± 0.017		2.936 ± 0.017	

^a From Minubayeva et al. [35]^b From Ryan et al. [26]^c Uncertainty calculated from the fitting parameters (Table 2)^d Uncertainty from standard deviation of average

Table 5 Experimental values of the first ionization constant of DL-norvaline, $pK_{a,COOH}$

t °C	$I \times 10^2$ mol·kg ⁻¹	Buffer ratio	Acridine indicator ratio	$pK_{a,COOH}$ results with Eq. 9 ^a		$pK_{a,COOH}$ results with Eq. 10 ^b	
				Experimental ^c	Average ^d	Experimental ^c	Average ^d
175.0 ± 0.1	4.967	15.29	0.8737	2.812 ± 0.007	2.811 ± 0.010	2.681 ± 0.007	2.680 ± 0.010
	4.986	12.19	1.066	2.824 ± 0.007		2.693 ± 0.007	
	4.965	10.12	1.324	2.811 ± 0.007		2.680 ± 0.007	
	5.024	5.044	2.750	2.796 ± 0.012		2.665 ± 0.012	
	4.974	15.55	0.5535	2.837 ± 0.008	2.830 ± 0.007	2.720 ± 0.008	2.714 ± 0.007
200.0 ± 0.1	4.995	12.43	0.6973	2.834 ± 0.008		2.717 ± 0.008	
	4.973	10.27	0.8430	2.834 ± 0.009		2.718 ± 0.009	
	5.032	5.084	1.769	2.818 ± 0.010		2.701 ± 0.010	
	5.005	3.041	2.880	2.829 ± 0.010		2.713 ± 0.010	
	4.962	15.11	0.3534	2.894 ± 0.008	2.894 ± 0.006	2.798 ± 0.008	2.797 ± 0.006
225.0 ± 0.1	4.982	12.10	0.4373	2.898 ± 0.008		2.801 ± 0.008	
	4.960	10.05	0.5295	2.896 ± 0.008		2.799 ± 0.008	
	5.021	5.024	1.053	2.899 ± 0.008		2.802 ± 0.008	
	4.992	3.009	1.829	2.881 ± 0.012		2.784 ± 0.012	
	4.975	15.57	0.2293	2.941 ± 0.011	2.960 ± 0.011	2.871 ± 0.011	2.891 ± 0.011
250.0 ± 0.1	4.995	12.40	0.2774	2.958 ± 0.010		2.888 ± 0.010	
	4.972	10.25	0.3309	2.964 ± 0.009		2.894 ± 0.009	
	5.035	5.095	0.6630	2.967 ± 0.009		2.897 ± 0.009	
	5.006	3.039	1.102	2.972 ± 0.008		2.902 ± 0.008	
	5.064	19.63	0.1176	3.000 ± 0.009	3.006 ± 0.008	2.968 ± 0.009	2.974 ± 0.008
275.0 ± 0.1	5.086	15.01	0.1494	3.013 ± 0.008		2.981 ± 0.008	
	5.062	12.01	0.1951	2.994 ± 0.010		2.962 ± 0.010	
	5.122	5.555	0.4063	3.010 ± 0.009		2.978 ± 0.009	

Table 5 continued

t °C	$I \times 10^2$ mol·kg ⁻¹	Buffer ratio	Acridine indicator ratio	p <i>K</i> _{a,COOH} results with Eq. 9 ^a		p <i>K</i> _{a,COOH} results with Eq. 10 ^b	
				Experimental ^c	Average ^d	Experimental ^c	Average ^d
5.100	3.255	0.6867	3.014 ± 0.009	2.982 ± 0.009			

^a From Minubayeva et al. [35]

^b From Ryan et al. [26]

^c Uncertainty calculated from the fitting parameters (Table 3)

^d Uncertainty from standard deviation of average

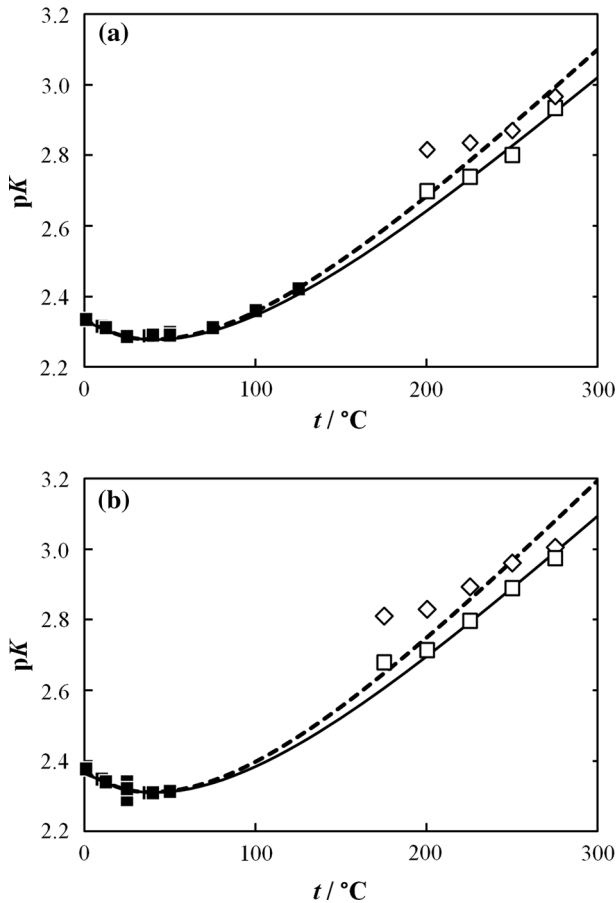


Fig. 4 Experimental values for the first ionization constant, $pK_{a,COOH}$ (Eq. 1), of **a** DL-2-aminobutyric acid and **b** DL-norvaline, plotted as a function of temperature. *Solid squares* correspond to data from the literature [16–19, 24, 38]. *Open points* show results from this study with acridine data from: *open diamonds*, Minubayeva et al. [35]; *open squares*, Ryan et al. [26]. *Lines* represent the extended van't Hoff fits (Eq. 29) obtained using $\Delta_r H_{a,COOH}^\circ$ from Christensen et al. [38] and K_{HAcr^+} from: *continuous line*, Ryan et al. [26] and *dashed line*, Minubayeva et al. [35]

3.2 Ionization Constant for the Ammonium Group, K_{a,NH_3^+}

Figures 5 and 6 show the spectra for 2-naphthoic acid at 275 °C and 4-nitrophenol at 175 °C, respectively, in their acid and basic extremes, along with the spectra for a series of DL-norvaline buffers. The fitting of Eq. 27 was done in the range between 300 and 380 nm, for 2-naphthoic acid, and 353 and 505 nm, for 4-nitrophenol. The values for the parameters k and l from these regressions obtained from each buffer ratio are shown in Tables 6 and 7.

Tables 8 and 9 show the ammonium ionization constants calculated using the regression results in Eq. 21. Figure S1 of the supplementary data shows our results for (a) pK_{a,NH_3^+} for DL-2-aminobutyric acid and (b) DL-norvaline, along with data at lower temperatures from

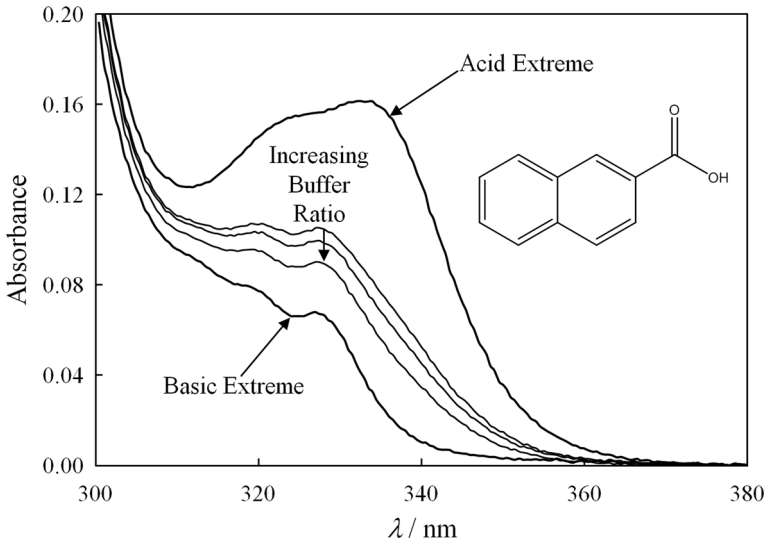


Fig. 5 UV-visible spectra of 2-naphthoic acid at 275 °C in HCl (acid extreme), NaOH (basic extreme) and DL-norvaline buffers. The buffer ratio A^-/HA^\pm increases in the direction of the arrow

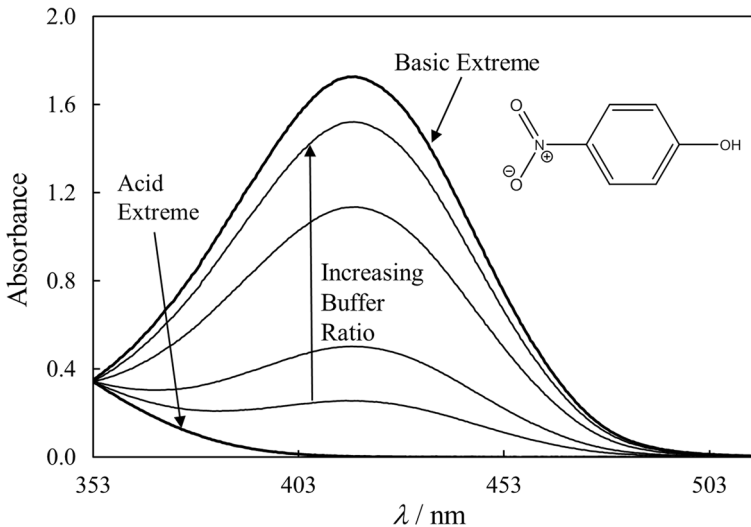


Fig. 6 UV-visible spectra of 4-nitrophenol at 175 °C in HCl (acid extreme), NaOH (basic extreme) and DL-norvaline buffers. The buffer ratio A^-/HA^\pm increases in the direction of the arrow

the literature [6, 15–19, 22, 23]. The values of pK_{a,NH_3^+} decrease as the temperature of the system increases.

The difference observed in the results of K_{a,NH_3^+} from 2-naphthoic acid and 4-nitrophenol at 200 °C suggest a systematic error in the values for one of these indicators. To quantify this, the ionization constant for DL-2-aminobutyric acid at 200 °C was determined with the two indicators in order to compare the results. This temperature was chosen

Table 6 The fitting parameters k and l for K_{a,NH_3^+} of DL-2-aminobutyric acid

$\frac{t}{^\circ C}$	D^a	Buffer ratio ^b	Indicator ratio ^c	k	l
175.0 ± 0.1^d	1.006	0.01532	7.861	0.8857 ± 0.0005	0.11268 ± 0.00005
	1.006	0.04327	3.238	0.7582 ± 0.0008	0.2342 ± 0.0001
	1.006	0.09777	1.402	0.5812 ± 0.0011	0.4144 ± 0.0001
	1.006	0.7096	0.1475	0.1249 ± 0.0011	0.8471 ± 0.0001
200.0 ± 0.1^d	1.010	0.01541	12.98	0.9731 ± 0.0003	0.07497 ± 0.00002
	1.010	0.09844	2.455	0.7367 ± 0.0004	0.30010 ± 0.00003
	1.010	0.1971	1.153	0.5522 ± 0.0004	0.47889 ± 0.00003
	1.010	0.7102	0.2858	0.2234 ± 0.0005	0.78158 ± 0.00004
200.0 ± 0.1^e	1.000	0.1045	0.06271	0.0591 ± 0.0015	0.9431 ± 0.0030
	1.004	0.1437	0.03433	0.0328 ± 0.0015	0.9547 ± 0.0029
225.0 ± 0.1^e	0.9982	0.1119	0.1372	0.1223 ± 0.0010	0.8914 ± 0.0020
	0.9982	0.2114	0.05781	0.0542 ± 0.0012	0.9380 ± 0.0024
	1.000	0.1323	0.09917	0.0891 ± 0.0021	0.8980 ± 0.0040
	1.000	0.3177	0.03730	0.0367 ± 0.0007	0.9849 ± 0.0014
250.0 ± 0.1^e	0.9992	0.1042	0.3306	0.2689 ± 0.0007	0.8133 ± 0.0014
	0.9992	0.2025	0.1433	0.1276 ± 0.0017	0.8905 ± 0.0030

^a Defined as m_{acid}^*/m_{base}^*

^b Defined as m_{A^-}/m_{HA^+}

^c Defined as m_{HInd}/m_{Ind}

^d 4-Nitrophenol as indicator

^e 2-Naphthoic acid as indicator

because the predicted value for the ionization constants fell in the optimum indicator range for both 2-naphthoic acid and 4-nitrophenol. These results, which appear in Table 8, show a difference of 0.5 log units between the two indicators, with a higher value of pK_{a,NH_3^+} obtained with 2-naphthoic acid. We chose to use the value obtained using 4-nitrophenol as the pH indicator, because it shows better agreement with the extrapolation from room temperature data, and because the ionization constants for 4-nitrophenol were determined more recently [36]. Based on these results, the ionization constant for 2-naphthoic acid was recalculated (see the Appendix), and these results were used to obtain new values for K_{a,NH_3^+} for both DL-2-aminobutyric acid and DL-norvaline at temperatures above 200 °C, which are also listed in Tables 8 and 9.

4 Thermodynamic Models

4.1 Extended van't Hoff Model for the Ionization Constant of the Carboxylic Acid Group

Our results were analyzed by the use of an extended van't Hoff equation [39], where the standard molar heat capacity for the reaction, $\Delta_r C_p^0$, was assumed to be constant in the

Table 7 The fitting parameters k and l for K_{a,NH_3^+} of DL-norvaline

$\frac{t}{^\circ\text{C}}$	D^a	Buffer ratio ^b	Indicator ratio ^c	k	l
175.0 ± 0.1^d	1.006	0.01743	5.845	0.8505 ± 0.0006	0.1455 ± 0.0001
	1.006	0.04768	2.441	0.7053 ± 0.0009	0.2890 ± 0.0001
	1.006	0.2308	0.4994	0.3278 ± 0.0013	0.6564 ± 0.0001
	1.006	0.8918	0.1159	0.1018 ± 0.0013	0.8785 ± 0.0001
200.0 ± 0.1^d	1.010	0.04775	4.114	0.8353 ± 0.0003	0.20304 ± 0.00003
	1.010	0.2307	0.8788	0.4786 ± 0.0004	0.54458 ± 0.00004
	1.010	0.8917	0.2232	0.1829 ± 0.0005	0.81938 ± 0.00004
225.0 ± 0.1^e	1.000	0.1165	0.1067	0.0996 ± 0.0007	0.9337 ± 0.0014
	1.000	0.1527	0.07806	0.0746 ± 0.0007	0.9554 ± 0.0014
	1.000	0.2198	0.05247	0.0512 ± 0.0007	0.9765 ± 0.0013
	1.000	0.3782	0.008723	0.0089 ± 0.0005	1.0251 ± 0.0010
	1.000	1.265	0.006287	0.0064 ± 0.0006	1.0214 ± 0.0011
250.0 ± 0.1^e	1.001	0.1351	0.2075	0.1754 ± 0.0011	0.8454 ± 0.0021
	1.001	0.1658	0.1647	0.1441 ± 0.0010	0.8745 ± 0.0020
	1.001	0.2349	0.1076	0.0985 ± 0.0011	0.9153 ± 0.0021
	1.001	0.3971	0.06282	0.0609 ± 0.0008	0.9701 ± 0.0015
	1.001	1.315	0.01469	0.0147 ± 0.0011	0.9999 ± 0.0021
275.0 ± 0.1^e	1.000	0.1228	0.5323	0.3663 ± 0.0012	0.6882 ± 0.0022
	1.000	0.1597	0.4047	0.3038 ± 0.0013	0.7507 ± 0.0024
	1.000	0.2280	0.2604	0.2136 ± 0.0016	0.8202 ± 0.0029

^a Defined as $m_{\text{acid}}^*/m_{\text{base}}^*$

^b Defined as $m_{\text{A}^-}/m_{\text{HA}^\pm}$

^c Defined as $m_{\text{HInd}}/m_{\text{Ind}}$

^d 4-Nitrophenol as indicator

^e 2-Naphthoic acid as indicator

whole temperature range studied. In this way, the expression for the first ionization constant for the amino acids can be written as

$$\ln K_{a,\text{COOH}}(T) = \ln K_{a,\text{COOH}}(T_r) - \frac{\Delta_r H_{a,\text{COOH}}^\circ(T_r)}{R} \left(\frac{1}{T} - \frac{1}{T_r} \right) + \frac{\Delta_r C_{pa,\text{COOH}}^\circ}{R} \left[\ln \frac{T}{T_r} + T_r \left(\frac{1}{T} - \frac{1}{T_r} \right) \right] \quad (29)$$

where T_r is the reference temperature, $T_r = 298.15$ K. For this assumption to be valid the reaction has to be chosen in such a way that $\Delta_r C_p^\circ$ is independent of temperature. “Iso-coulombic” (charge symmetric) reactions are known to have small and almost constant values for $\Delta_r C_p^\circ$ over a wide range of temperature [40], consistent with this assumption, and are a good choice when using this model.

Table 8 Experimental values of pK_{a,NH_3^+} of DL-2-aminobutyric acid

t °C	$I \times 10^2$ mol·kg ⁻¹	Buffer ratio	Indicator ratio	pK_{a,NH_3^+}	
				Experimental ^a	Average ^b
175.0 ± 0.1 ^c	5.182	0.01532	7.861	7.325 ± 0.001	7.310 ± 0.051
	5.400	0.04327	3.238	7.259 ± 0.001	
	5.250	0.09777	1.402	7.268 ± 0.001	
	5.296	0.7096	0.1475	7.386 ± 0.003	
200.0 ± 0.1 ^{c,d}	5.181	0.01541	12.98	7.139 ± 0.001	7.103 ± 0.034
	5.244	0.09844	2.455	7.056 ± 0.001	
	5.295	0.1971	1.153	7.083 ± 0.001	
	5.293	0.7102	0.2858	7.132 ± 0.001	
200.0 ± 0.1 ^{e,d}	4.913	0.1045	0.06271	7.532 ± 0.013	7.594 ± 0.062
	5.115	0.1437	0.03433	7.655 ± 0.022	
225.0 ± 0.1 ^e	4.901	0.1119	0.1372	7.518 ± 0.004	7.588 ± 0.044
	4.968	0.2114	0.05781	7.618 ± 0.011	
	5.150	0.1323	0.09917	7.587 ± 0.012	
	5.041	0.3177	0.03730	7.631 ± 0.009	
250.0 ± 0.1 ^e	4.925	0.1042	0.3306	7.539 ± 0.002	7.576 ± 0.037
	4.992	0.2025	0.1433	7.614 ± 0.007	
200.0 ± 0.1 ^f	4.913	0.1045	0.06271	7.041 ± 0.013	7.102 ± 0.062
	5.115	0.1437	0.03433	7.164 ± 0.022	
225.0 ± 0.1 ^f	4.901	0.1119	0.1372	6.929 ± 0.004	6.999 ± 0.044
	4.968	0.2114	0.05781	7.028 ± 0.011	
	5.150	0.1323	0.09917	6.997 ± 0.012	
	5.041	0.3177	0.03730	7.041 ± 0.009	
250.0 ± 0.1 ^f	4.925	0.1042	0.3306	6.868 ± 0.002	6.906 ± 0.037
	4.992	0.2025	0.1433	6.943 ± 0.007	

^a Uncertainty calculated from the fitting parameters (Table 6)

^b Uncertainty from standard deviation of average

^c 4-Nitrophenol as indicator (Ehlerova et al. [36])

^d Data used for the recalculation of $K_{2-NaphCOOH}$ (see text)

^e 2-Naphthoic acid as indicator (Xiang and Johnston [28])

^f 2-Naphthoic acid as indicator (recalculated, see text)

The first ionization reactions, Eq. 1, for the α -amino acids used in this study are iso-coulombic, as shown in Fig. 1a, considering the zwitterion as a neutral species. Hence, Eq. 29 was fitted with the values of $K_{a,COOH}$ for DL-2-aminobutyric acid from Smith et al. [16], Christensen et al. [38], Wang et al. [24] and our experimental values in Table 4 at (225, 250 and 275) °C. Likewise, for DL-norvaline, Eq. 29 was fitted with the data from Smith et al. [16], Christensen et al. [38] and our results listed in Table 5 at (200, 225, 250 and 275) °C. Our data at 200 °C for DL-2-aminobutyric acid and 175 °C for DL-norvaline were not included in the fit because they were too close to the limits of the effective indicator range.

Table 9 Experimental values of pK_{a,NH_3^+} of DL-norvaline

t °C	$I \times 10^2$ mol·kg ⁻¹	Buffer ratio	Indicator ratio	pK_{a,NH_3^+}	
				Experimental ^a	Average ^b
175.0 ± 0.1 ^c	5.260	0.01743	5.845	7.397 ± 0.001	7.368 ± 0.030
	5.298	0.04768	2.441	7.340 ± 0.001	
	5.344	0.2308	0.4994	7.344 ± 0.002	
	5.245	0.8918	0.1159	7.391 ± 0.005	
200.0 ± 0.1 ^c	5.298	0.04775	4.114	7.147 ± 0.001	7.140 ± 0.007
	5.344	0.2307	0.8788	7.133 ± 0.001	
	5.245	0.8917	0.2232	7.141 ± 0.001	
225.0 ± 0.1 ^d	5.007	0.1165	0.1097	7.610 ± 0.004	7.627 ± 0.016
	5.044	0.1527	0.07386	7.628 ± 0.005	
	4.995	0.2198	0.04922	7.643 ± 0.006	
250.0 ± 0.1 ^d	4.955	0.1351	0.2075	7.628 ± 0.004	7.655 ± 0.025
	5.008	0.1658	0.1647	7.640 ± 0.004	
	4.959	0.2349	0.1076	7.673 ± 0.006	
	5.051	0.3971	0.06282	7.679 ± 0.006	
275.0 ± 0.1 ^d	4.989	0.1228	0.5323	7.656 ± 0.003	7.671 ± 0.023
	5.025	0.1597	0.4047	7.660 ± 0.003	
	4.975	0.2280	0.2604	7.697 ± 0.005	
225.0 ± 0.1 ^e	5.007	0.1165	0.1097	7.021 ± 0.004	7.038 ± 0.016
	5.044	0.1527	0.07386	7.039 ± 0.005	
	4.995	0.2198	0.04922	7.053 ± 0.006	
250.0 ± 0.1 ^e	4.955	0.1351	0.2075	6.958 ± 0.004	6.984 ± 0.025
	5.008	0.1658	0.1647	6.969 ± 0.004	
	4.959	0.2349	0.1076	7.003 ± 0.006	
	5.051	0.3971	0.06282	7.008 ± 0.006	
275.0 ± 0.1 ^e	4.989	0.1228	0.5323	6.913 ± 0.003	6.928 ± 0.023
	5.025	0.1597	0.4047	6.918 ± 0.003	
	4.975	0.2280	0.2604	6.954 ± 0.005	

^a Uncertainty calculated from the fitting parameters (Table 7)

^b Uncertainty from standard deviation of average

^c 4-Nitrophenol as indicator (Ehlerova et al. [36])

^d 2-Naphthol acid as indicator (Xiang and Johnston [28])

^e 2-Naphthoic acid as indicator (recalculated, see text)

Two different fits were tried for each series. In the first approach, both the values for $\Delta_r H_{a,COOH}^\circ$ at 25 °C and $\Delta_r C_{p a,COOH}^\circ$ were obtained from the fitting. In the second, the value for $\Delta_r H_{a,COOH}^\circ$ was fixed to the literature values from Smith et al. [16], leaving $\Delta_r C_{p a,COOH}^\circ$ as the only fitting parameter. In order to choose between the values for $K_{a,COOH}$ obtained with the two expressions for the ionization constant of acridine, both sets of data were fitted using the model. These results are listed in Table 10 and plotted in Fig. 4.

Table 10 Values for $\Delta_r H_{a,COOH}^{\circ}(25^{\circ}C)$ and $\Delta_r C_{pa,COOH}^{\circ}$ for the first ionization reaction, $H_2A^+(aq) \rightleftharpoons HA^{\pm}(aq) + H^+(aq)$

Amino acid	$\log_{10} K_{a,COOH}(25^{\circ}C)^a$	$\frac{\Delta_r H_{a,COOH}^{\circ}(25^{\circ}C)}{kJ \cdot mol^{-1}}$	$\frac{\Delta_r C_{pa,COOH}^{\circ}}{J \cdot K^{-1} \cdot mol^{-1}}$	$\sigma(\log_{10} K_{a,COOH})$
<i>DL-2-Aminobutyric acid</i>				
Extended van't Hoff model ^c , pK_{HAcr^+} from Ryan et al. [26]				
2 Parameters	-2.286 ± 0.005^a	1.26 ± 0.25^c	-91.9 ± 3.0^c	0.011
1 Parameter	-2.286 ± 0.005^a	1.59 ± 0.21^d	-95.7 ± 1.0^c	0.012
Extended van't Hoff Model ^b , pK_{HAcr^+} from Minubayeva et al. [35]				
2 Parameters	-2.286 ± 0.005^a	1.31 ± 0.40^c	-101.1 ± 4.8^c	0.018
1 Parameter	-2.286 ± 0.005^a	1.59 ± 0.21^d	-104.2 ± 1.5^c	0.018
<i>DL-Norvaline</i>				
Extended van't Hoff model ^b , pK_{HAcr^+} from Ryan et al. [26]				
2 Parameters	-2.286 ± 0.005^a	1.59 ± 0.35^c	-100.2 ± 4.0^c	0.011
1 Parameter	-2.286 ± 0.005^a	1.63 ± 0.17^d	-100.6 ± 0.8^c	0.010
Extended van't Hoff model ^b , pK_{HAcr^+} from Minubayeva et al. [35]				
2 Parameters	-2.286 ± 0.005^a	0.02 ± 1.25^c	-93.7 ± 14.2^c	0.038
1 Parameter	-2.286 ± 0.005^a	1.63 ± 0.17^d	-111.6 ± 3.0^c	0.039

^a From Smith et al. [16]

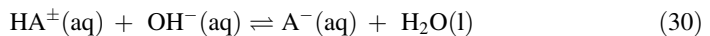
^b From Eq. 29

^c Fitted parameter

^d $\Delta_r H_{a,COOH}^{\circ}$ From Christensen et al. [38]

4.2 Extended van't Hoff Model for the Ionization Constant of the Ammonium Group

The second ionization reaction for the amino acids, Eq. 3, is not isocoulombic as written. The equivalent isocoulombic reaction is



with

$$K_{a,OH,NH_3^{\pm}} = \frac{K_{a,NH_3^{\pm}}}{K_w} = \frac{m_{A^-}}{m_{HA^{\pm}} m_{OH^-}} \frac{\gamma_{A^-}}{\gamma_{HA^{\pm}} \gamma_{OH^-}} \tag{31}$$

where we have assumed that $\gamma_{A^-} \approx \gamma_{OH^-}$ and $\gamma_{HA^{\pm}} \approx 1$. Equation 29 was fitted to the results for $K_{a,OH,NH_3^{\pm}}$ obtained from this work, along with reported values from Smith et al. [16], Anderson et al. [22], and Gillespie et al. [23] for DL-2-aminobutyric acid, and from Smith et al. [16] for DL-norvaline. Data for the ionization constant of water, K_w , were taken from Sweeton et al. [41]. As was done for the first ionization constant, Eq. 29 was fitted to the data with and without fixing the value for $\Delta_r H_{a,OH,NH_3^{\pm}}^{\circ}$ to the literature value reported by Smith et al. [16]. These results are shown in Fig. 7. Values for $\Delta_r H_{a,NH_3^{\pm}}^{\circ}$ and $\Delta_r C_{pa,NH_3^{\pm}}^{\circ}$ calculated from these results are shown in Table 11.

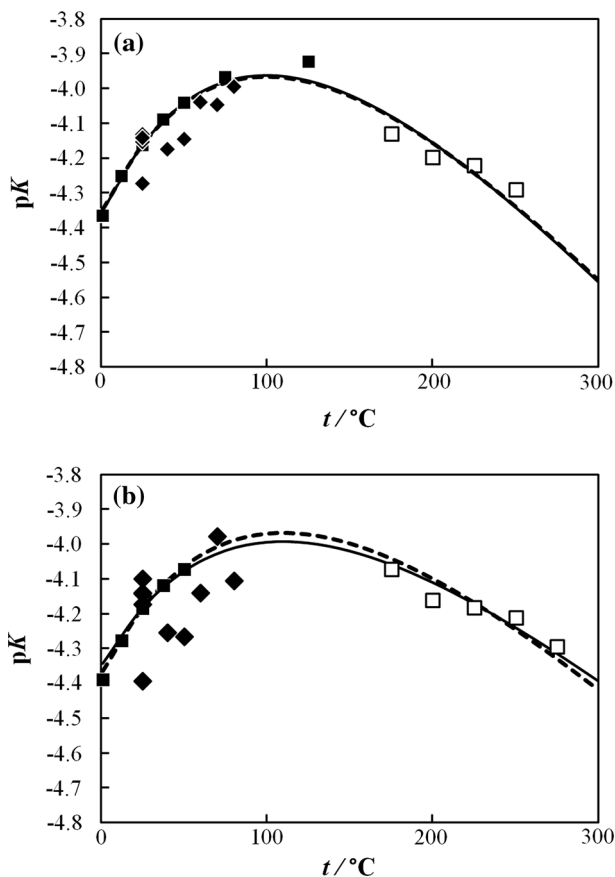


Fig. 7 Experimental values for the isocoulombic form of the second ionization constant, pK_{a,OH,NH_3^+} (Eq. 30), of **a** DL-2-aminobutyric acid and **b** DL-norvaline plotted as a function of temperature. *Solid points* correspond to data from literature. *Open points* show results from this study. *Squares*, data included in the fit [16, 22, 23]; *diamonds*, data not included in the fit [6, 15, 17–19]. *Lines* represent the extended van't Hoff fits (Eq. 29) with: *dashed line*, one parameter; *continuous line*, two calculated parameters

5 Discussion

5.1 Comparison with Literature Data

The plots of our experimental values of $K_{a,COOH}$ for DL-2-aminobutyric acid and DL-norvaline in Fig. 4 suggest that the values calculated from the pK_{HAcr^+} data for acridine from Ryan et al. [26] are more consistent with low-temperature literature results than those from Minubayeva et al. [35]. This can be tested by comparing the results for $\Delta_r H_{a,COOH}^{\circ}$ and $\Delta_r C_p^{\circ}$ obtained from fitting Eq. 29 with the values of $K_{a,COOH}$ in Table 10, with the critically evaluated values near 25 °C from Christensen et al. [38] and the more recent experimental values from (50 to 125) °C reported by Wang et al. [24]; Christensen's values of $\Delta_r H_{a,COOH}^{\circ} = (1.59 \pm 0.21) \text{ kJ}\cdot\text{mol}^{-1}$ for DL-2-aminobutyric acid and $(1.63 \pm 0.17) \text{ kJ}\cdot\text{mol}^{-1}$ for DL-norvaline [38] at 25 °C agree with the values in Table 10,

Table 11 Values for $\Delta_r H_{a,\text{NH}_3^+}^\circ$ (25 °C) and $\Delta_r C_{p\ a,\text{NH}_3^+}^\circ$ for the second ionization reaction, $\text{HA}^\pm(\text{aq}) \rightleftharpoons \text{A}^-(\text{aq}) + \text{H}^+(\text{aq})$

Amino acid	$\log_{10} K_{a,\text{NH}_3^+}$ (25 °C) ^a	$\Delta_r H_{a,\text{NH}_3^+}^\circ$ (25 °C) kJ·mol ⁻¹	$\Delta_r C_{p\ a,\text{NH}_3^+}^\circ$ J·K ⁻¹ ·mol ⁻¹	$\sigma(\log_{10} K_{a,\text{NH}_3^+})$
DL-2-aminobutyric acid	-9.83 ± 0.04			
Extended van't Hoff model ^b				
2 Parameters		45.2 ± 0.9 ^{c,c}	-89.8 ± 13.6 ^{d,c}	0.036
1 Parameter		45.4 ± 0.4 ^{a,c}	-92.6 ± 6.9 ^{d,c}	0.034
DL-norvaline	-9.808 ± 0.04			
Extended van't Hoff model ^b				
2 Parameters		46.7 ± 0.9 ^{c,c}	-124.2 ± 12.1 ^{d,c}	0.028
1 Parameter		45.52 ± 0.40 ^{a, c}	-110.3 ± 6.7 ^{d,c}	0.030

^a From Smith et al. [16]

^b From fitting of Eq. 29 to $K_{a,\text{OH},\text{NH}_3^+}$ for the isocoulombic reaction, Eq. 31; $K_{a,\text{NH}_3^+} = K_{a,\text{OH},\text{NH}_3^+} + K_w$ (K_w taken from Sweeton et al. [41])

^c $\Delta_r H_{a,\text{NH}_3^+}^\circ = \Delta_r H_{a,\text{OH},\text{NH}_3^+}^\circ + \Delta_r H_w^\circ$ ($\Delta_r H_w^\circ$ (25 °C) from Sweeton et al. [41])

^d $\Delta_r C_{p\ a,\text{NH}_3^+}^\circ = \Delta_r C_{p\ a,\text{OH},\text{NH}_3^+}^\circ + \Delta_r C_{p\ w}^\circ$ ($\Delta_r C_{p\ w}^\circ$ from Sweeton et al. [41])

^e Fitted parameter

calculated using the data for acridine from Ryan et al. [26], $\Delta_r H_{a,\text{COOH}}^\circ = (1.26 \pm 0.25)$ kJ·mol⁻¹ for DL-2-aminobutyric acid and $\Delta_r H_{a,\text{COOH}}^\circ = (1.59 \pm 0.35)$ kJ·mol⁻¹ for DL-norvaline, to within the combined experimental uncertainties. These results compare with the value $\Delta_r H_{a,\text{COOH}}^\circ = (1.31 \pm 0.40)$ kJ·mol⁻¹ for DL-2-aminobutyric acid and $\Delta_r H_{a,\text{COOH}}^\circ = (0.02 \pm 1.25)$ kJ·mol⁻¹ for DL-norvaline, calculated using the acridine data from Minubayeva et al. [35]. Moreover, the standard errors of $\log_{10} K_{a,\text{COOH}}$ for all regressions when using the values from Ryan et al. [26], $\sigma(\log_{10} K_{a,\text{COOH}}) \leq 0.012$, are smaller than those obtained using values from Minubayeva et al. [35] { $\sigma(\log_{10} K_{a,\text{COOH}}) = 0.018$ for DL-2-aminobutyric acid and 0.04 for DL-norvaline}. Based on these results, we consider our values for $K_{a,\text{COOH}}$, obtained with the data for acridine from Ryan et al. [26], to be more accurate, and they are used in the rest of the analysis.

It is also interesting to note that the fits of Eq. 29 to the amino acid ionization constants using indicator data from Ryan et al. [26] with one or two adjustable parameters are so close that the plots in Fig. 4 are indistinguishable. Differences in the standard error of $\log_{10} K_{a,\text{COOH}}$ of the regressions are less than ±0.001 for both amino acids, and the differences between the results for $\Delta_r C_{p\ a,\text{COOH}}^\circ$ obtained from the two regressions are smaller than the combined uncertainties. For consistency with the literature, we chose to use in the results obtained with $\Delta_r C_{p\ a,\text{COOH}}^\circ$ as the only fitted parameter for both amino acids.

Wang et al. [24] have reported values for $\Delta_r C_{p\ a,\text{COOH}}^\circ$ for DL-2-aminobutyric acid and DL-norvaline obtained from literature data and their flow calorimetric measurements at temperatures from 50 to 125 °C. The mean value for DL-2-aminobutyric acid from their results over the range 25–125 °C is $\Delta_r C_p^\circ = (-99 \pm 10)$ J·K⁻¹·mol⁻¹, which agrees with the value obtained in this study, (-95.7 ± 1.0) J·K⁻¹·mol⁻¹, to within the combined

experimental uncertainties. Our value for DL-norvaline, $\Delta_r C_{pa,COOH}^\circ = (-100.6 \pm 0.8) \text{ J}\cdot\text{K}^{-1}\cdot\text{mol}^{-1}$, agrees with the value at 25 °C reported by Christensen et al. [38], $(-125 \pm 25) \text{ J}\cdot\text{K}^{-1}\cdot\text{mol}^{-1}$, to within the combined experimental uncertainties.

Results for the fitting of Eq. 29 to the second ionization constants of the amino acids are listed in Table 11. The values obtained for DL-2-aminobutyric acid show no significant difference for $\Delta_r H_{a,NH_3^+}^\circ$ at 25 °C by the two fits. However, the value for $\Delta_r C_{pa,NH_3^+}^\circ$, obtained with the fixed value for $\Delta_r H_{a,NH_3^+}^\circ$ from Smith et al. [16], has a smaller uncertainty. In the case of DL-norvaline, the difference between the 1- and 2-parameter fits is $1.18 \text{ kJ}\cdot\text{mol}^{-1}$, slightly smaller than the combined uncertainties of $\pm 0.9 \text{ kJ}\cdot\text{mol}^{-1}$ and $\pm 0.40 \text{ kJ}\cdot\text{mol}^{-1}$. As for the first ionization reaction, the results obtained using $\Delta_r C_{pa,NH_3^+}^\circ$ as the only fitted parameter were used in our analysis.

Gillespie et al. [23] reported values for $\Delta_r C_{pa,NH_3^+}^\circ$ obtained from isothermal flow mixing calorimetric measurements. Their results give a constant value of $\Delta_r C_{pa,NH_3^+}^\circ = (-80 \pm 10) \text{ J}\cdot\text{K}^{-1}\cdot\text{mol}^{-1}$ for the temperature range between 50 and 125 °C. This value agrees with our value of $(-97.1 \pm 7.2) \text{ J}\cdot\text{K}^{-1}\cdot\text{mol}^{-1}$ within the combined experimental uncertainty. No direct experimental results for $\Delta_r C_{pa,NH_3^+}^\circ$ were found in literature.

5.2 Thermodynamic Analysis

The values of $pK_{a,COOH}$ for the amino acids shown in Fig. 4 pass through a minimum at about 50° C and then increase at higher temperatures. This is consistent with results from Wang et al. [24] and Clarke et al. [25] for these and other α -amino acids at temperatures up to 125 °C. The corresponding values for the second ionization constants, pK_{a,NH_3^+} , measured by Gillespie et al. [23] and Clarke et al. [25], decrease systematically from (25 to 125) °C. Our results for pK_{a,NH_3^+} of DL-2-aminobutyric acid and DL-norvaline show similar trends which extend to much higher temperatures, (250 and 275) °C respectively, as can be seen in Fig. S1 of the supplementary data.

Values for the standard molar enthalpy and entropy of reaction at each temperature can be calculated from the fitted values of $\Delta_r H_a^\circ(T_r)$ and $\Delta_r C_{pa}^\circ$ in Tables 10 and 11 [39]:

$$\Delta_r H_a^\circ(T) = \Delta_r H_a^\circ(T_r) + \Delta_r C_{pa}^\circ (T - T_r) \quad (32)$$

$$\Delta_r S_a^\circ(T) = \Delta_r S_a^\circ(T_r) + \Delta_r C_{pa}^\circ \ln(T/T_r) \quad (33)$$

The results for $\Delta_r H_a^\circ$ and $-\Delta_r S_a^\circ$ obtained from Eqs. 32 and 33 for the first and second ionization equilibria are shown in Fig. 8, along with data from literature [16, 22–24, 38]. The differences between the two amino acids are less than $5 \text{ kJ}\cdot\text{mol}^{-1}$ over the entire temperature range studied. This is true for both ionization reactions.

The factors controlling the temperature dependence of proton ionization reactions have been discussed by Kay [42], Mesmer [40], Tremaine and Arcis [43] and others. Briefly, ionization reactions are driven by opposing enthalpic and entropic effects. Enthalpic effects are associated with the breakup or formation of strong hydrogen bonds in the reactants or products. At low temperatures, entropic effects are associated with the ionic hydration of the reactants and products, the so-called “structure making” and “structure breaking” effects [42]. At high temperatures, the dominant entropic effect is the formation of an

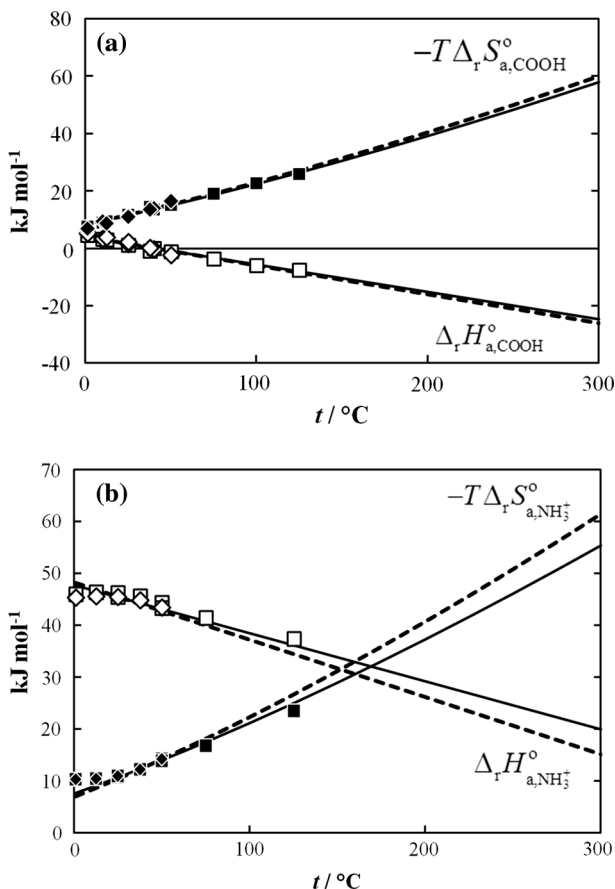


Fig. 8 Values for **a** $\Delta_r H_{a,COOH}^\circ$ and $-T\Delta_r S_{a,COOH}^\circ$; **b** $\Delta_r H_{a,NH_3^+}^\circ$ and $-T\Delta_r S_{a,NH_3^+}^\circ$ for: *continuous lines*, DL-2-aminobutyric acid and *dashed lines*, DL-norvaline, calculated with Eqs. 34 and 35. Points correspond to literature data [16, 22–24, 38] for $\Delta_r H_a^\circ$ (open points) and $-T\Delta_r S_a^\circ$ (solid points): squares, DL-2-aminobutyric acid; diamonds, DL-norvaline

increasingly large hydration sphere due to ion–dipole interactions associated with the much higher compressibility of liquid water as the critical point is approached [40, 43, 44].

The temperature dependence of $K_{a,COOH}$ and K_{a,NH_3^+} for amino acid ionization reactions has been discussed by Wang et al. [24], Gillespie et al. [23] and Clarke et al. [25]. For the first ionization reaction, the increase in $pK_{a,COOH}$ between (25 and 300) °C is ~ 0.8 units, smaller than the increase of ~ 1.5 units for acetic acid and other carboxylic acids [45]. The value of $\Delta_r H_{a,COOH}^\circ$ at $t = 0$ °C, shown in Fig. 8, is small but positive and $\Delta_r H_{a,COOH}^\circ \approx -T\Delta_r S_{a,COOH}^\circ$, as expected for an isocoulombic reaction [40]. The decrease in $\Delta_r H_{a,COOH}^\circ$ from positive to negative values at temperatures above ~ 50 °C is associated with the shallow minimum in the plot of $pK_{a,COOH}$ shown in Fig. 4. The increase in the negative enthalpic contribution with temperature is offset by an even larger entropic contribution, $\Delta_r H_{a,COOH}^\circ < -T\Delta_r S_{a,COOH}^\circ$. The results show that the zwitterion AH^\pm and hydronium ion become increasingly less stable than the protonated species AH_2^+ at

temperatures above 100 °C, and that this is primarily due to entropic effects. Clarke and Tremaine [30] have noted that dipole–solvent polarization has a significant effect on the thermodynamic properties of the amino acid's zwitterion in high temperature water, making it less stable. While this effect is smaller than the ion–solvent polarizations of the protonated reactant species AH_2^+ and the hydronium ion product H_3O^+ , the effects of the two ions cancel because reaction (1) is isocoulombic. We speculate that much of the slight increase in $\text{p}K_{\text{a,COOH}}$ with increasing temperature may be due to solvent polarization by the dipole of AH^+ .

The second ionization reaction is endothermic over the whole range of temperatures, and $\text{p}K_{\text{a,NH}_3^+}$ decreases by ~ 4.0 units between (25 and 300) °C, similar to the decrease observed for most amine ionization reactions [45]. Amines are unusual in that $\text{p}K_{\text{a,NH}_3^+}$ for the isocoulombic acid ionization reactions of $\text{RNH}_2^+(\text{aq}) \rightleftharpoons \text{RNH}(\text{aq}) + \text{H}^+(\text{aq})$ decreases dramatically with increasing temperature, rather than increasing as much as expected from the solvent polarization arguments mentioned above. Presumably, this is caused by the extensive hydrogen bonding to the ammonium ion, even at elevated temperatures. Moreover, the presence of the carboxylate group in the amino acid zwitterion does not seem to exert a major effect on $\text{p}K_{\text{a,NH}_3^+}$ relative to simple alkyl amines [45]. These effects are discussed in the following section.

5.3 Comparison with the SOCW Functional Group Additivity model

Functional group additivity schemes are based on the assumption that a thermodynamic property of organic solutes can be calculated as a sum of contributions of the different functional groups that form the molecule [11]. In general, the equation for calculating a thermodynamic property for a compound with this scheme is

$$Y_2^{\circ} = (1 - z)(Y_{\text{ss}} - A_Y) + \sum_{i=1}^N n_i Y_{2,i}^{\circ} \quad (34)$$

where N is the total number of functional groups, n_i is the number of occurrences of each specific functional group, Y_2° is the thermodynamic property of the compound, $Y_{2,i}^{\circ}$ is the contribution to the property by each functional group, z is the charge of the particle, Y_{ss} is a standard state term, and A_Y is a conversion factor, which depends on the standard state chosen. The term $(1 - z)$ accounts for the hydrogen convention scale, $Y_{2,\text{H}^+}^{\circ} = 0$. Group additivity models for standard thermodynamic properties of aqueous solutions of organic solutes, at high temperatures and pressures, have been reported by Amend and Helgeson [10] and Yezdimer et al. [11]. In the discussion below, we focus on the treatment by Yezdimer et al. [11], whose model is based on the functional group contributions to terms in the equation of state proposed by Sedlbauer et al. [14].

In developing their model, Yezdimer et al. [11] determined that a simple combination of the COO^- and NH_3^+ groups was insufficient to predict the properties for amino acids. For this reason, a functional group $Y_{2,\text{AMINO}}^{\circ}$, specific to the zwitterionic form of the amino

acids, $^-\text{OOC} - \overset{\text{O}}{\underset{\text{O}}{\text{C}}} - \text{NH}_3^+$, was proposed. The expression for the standard molar properties of the first ionization reaction is:

$$\Delta_r Y_{2a,COOH}^o = Y_{2AMINO}^o - (Y_{2COOH}^o + Y_{2NH_3^+}^o) \tag{35}$$

where the subscript AMINO refers to the contribution from the amino acid group. Likewise, for the second ionization, the equation is

$$\Delta_r Y_{2a,NH_3^+}^o = (Y_{2COO^-}^o + Y_{2NH_2}^o) - Y_{2AMINO}^o \tag{36}$$

As is true for any functional group additivity model, the values of $\Delta_r V_{2a}^o$ and $\Delta_r C_{pa}^o$ for each ionization reaction must be equal for all amino acids. Equilibrium constants were calculated from the generalized form of Eq. 29,

$$\begin{aligned} \ln K_a(T) = \ln K_a(T_r) - \frac{\Delta_r H_a^o(T_r)}{R} \left(\frac{1}{T} - \frac{1}{T_r} \right) + \frac{1}{R} \int_{298.15}^T \frac{\Delta_r C_p^o}{T} dT - \frac{1}{RT} \int_{298.15}^T \Delta_r C_p^o dT \\ - \frac{1}{RT} \int_1^p \Delta_r V^o dp. \end{aligned} \tag{37}$$

Differences in the temperature dependence of the two ionization constants between different amino acids can arise only from difference in the enthalpies of reaction, $\Delta_r H_a^o(T_r)$.

Values for the thermodynamic properties $\Delta_r V_{2a}^o$, $\Delta_r C_{pa}^o$, $\Delta_r H_a^o$, $\Delta_r H_a^o$, $\Delta_r S_a^o$, $\Delta_r G_a^o$ and pK_a for the first and second ionization reactions of glycine, 2-alanine, 2-aminobutyric acid and norvaline were calculated at temperatures from (0.0 to 300.0) °C and a pressure of 10 MPa from the available literature data at 25 °C [5, 16, 21, 23, 24, 38, 46–50] (listed in Tables S1–S3 of the supplementary material) through the use of Yezdimer et al.’s SOCW functional group additivity model. These results appear in Tables S4–S6 of the supplementary material. A comparison of the difference between predicted results for the first and second ionization constants with the corresponding experimental values is presented in Fig. 9. This figure plots the differences in pK_a , expressed as $\Delta pK_a = pK_{a,Exp} - pK_{a,Pred}$ between the predictions and experimental data from this work and other studies [5, 6, 16, 18, 19, 23–25] the four amino acids at temperatures up to 225 °C.

The left side (a) of Fig. 9 shows the differences in the first ionization constant, $\Delta pK_{a,COOH}$. At 25 °C the model agrees well with experimental data for the first ionization (highest $\Delta pK_{a,COOH}$ of 0.06). As temperature increases, the predictions from the model deviate more from the experimental results, with differences at 250 °C of up to 0.59 for norvaline (this work) and 0.70 for glycine (Clarke et al. [25]). These deviations are very similar for all four amino acids.

The right side (b) of Fig. 9 shows the values of $\Delta pK_{a,NH_3^+}$ for the second ionization reaction. The functional group additivity model shows good agreement at 25 °C with the data from Smith et al. [16], Clarke et al. [25], Hamborg et al. [5] and our regression from the extended van’t Hoff model ($|\Delta pK_{a,NH_3^+}| < 0.02$), but agrees less well with the data from Gergely and Sovago [18], Gergely et al. [19] or Yang et al. [6] ($|\Delta pK_{a,NH_3^+}| < 0.34$). At temperatures up to 125 °C, the temperature-dependant ionization constants predicted by the model are in good agreement with the literature data [5, 23] ($|\Delta pK_{a,NH_3^+}| \leq 0.11$), except for the values reported for glycine by Clarke et al. [25], which are also the only ones that show more positive values for pK_{a,NH_3^+} than the ones obtained from the model. At

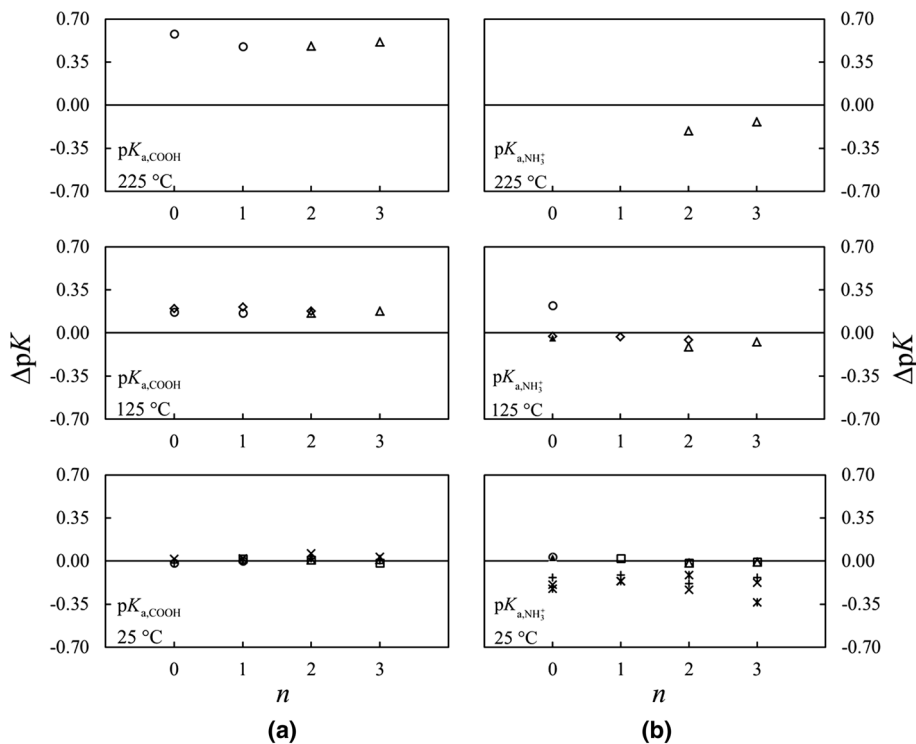


Fig. 9 ΔpK_a , defined as $\Delta pK_a = pK_{a,Exp} - pK_{a,Pred}$, versus number of carbons of the side chain for the **a** first and **b** second ionization constants of the amino acids (0 = glycine, 1 = 2-alanine, 2 = 2-aminobutyric acid, 3 = norvaline) at $t = 25\text{ }^\circ\text{C}$ (bottom), $t = 125\text{ }^\circ\text{C}$ (middle) and $t = 225\text{ }^\circ\text{C}$ (top). Predicted values from Yezdimer et al. [11]. Experimental data from: open squares, Smith et al. [16]; open diamonds, a Wang et al. [24] and b Gillespie et al. [23]; open circles, Clarke et al. [25]; X, Gergely and Sovago [18]; plus signs, Gergely et al. [19]; asterisks, Yang et al. [6]; filled diamond, Hamborg et al. [5]; open diamond, this work

higher temperatures, the results from our current study are the only values available for comparison. The model predictions have larger deviations than the values at lower temperatures ($|\Delta pK_{a,NH_3^+}| < 0.27$) but show better agreement than those for the first ionization reaction. As for the lower temperatures, the predicted values of pK_{a,NH_3^+} are larger than the experimental values, and similar for both amino acids.

Figure 10 compares the results for $\Delta_r H_{a,COOH}^0$ and $-T\Delta_r S_{a,COOH}^0$ from this study and the literature with those from the functional group additivity model. The model is in reasonable agreement with experimental data up to about $50\text{ }^\circ\text{C}$, where the predicted values begin to show a different trend. Since the experimental values of $\Delta_r H_{a,COOH}^0$ at $25\text{ }^\circ\text{C}$ (Table 10) are the same as those used in the group additivity model, the difference between them at elevated temperatures arises from the model predictions for $\Delta_r C_p^0$. The prediction for the average value of $\Delta_r C_p^0$ for the temperature range $0\text{ }^\circ\text{C} \leq t \leq 125\text{ }^\circ\text{C}$ for all 2-amino acids is $-29.05\text{ J}\cdot\text{mol}^{-1}\cdot\text{K}^{-1}$, smaller in magnitude than the values for 2-aminobutyric acid from literature $\Delta_r C_p^0 = (-99.9 \pm 10)\text{ J}\cdot\text{K}^{-1}\cdot\text{mol}^{-1}$ [24] and for DL-2-aminobutyric acid and DL-norvaline from this work, $\Delta_r C_p^0 = (-95.7 \pm$

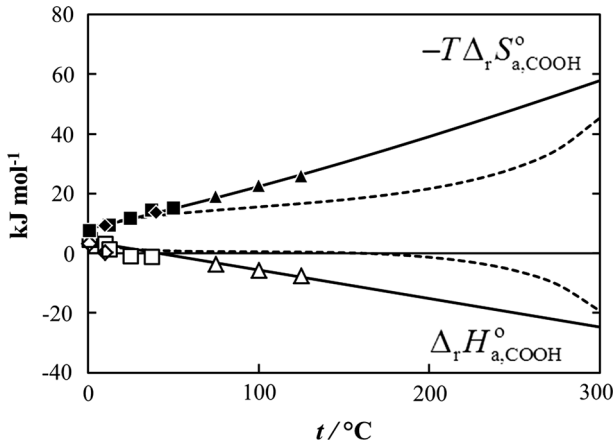


Fig. 10 Comparison between results for $\Delta_r H_{a,\text{COOH}}^\circ$ and $-T\Delta_r S_{a,\text{COOH}}^\circ$ for DL-2-aminobutyric acid obtained from the extended van't Hoff model and the predicted results from group additivity: *continuous lines*, calculated with Eq. 32 ($\Delta_r H_{a,\text{COOH}}^\circ$) or Eq. 33 ($-T\Delta_r S_{a,\text{COOH}}^\circ$); *dashed lines*, predicted with the group additivity model (Yezdimer et al. [11]). *Points* correspond to data from the literature. *Open points*: $\Delta_r H_{a,\text{COOH}}^\circ$; *solid points*: $-T\Delta_r S_{a,\text{COOH}}^\circ$. Data from: *squares*, Smith et al. [16]; *diamonds*, Christensen et al. [38] and *triangles*, Wang et al. [24]

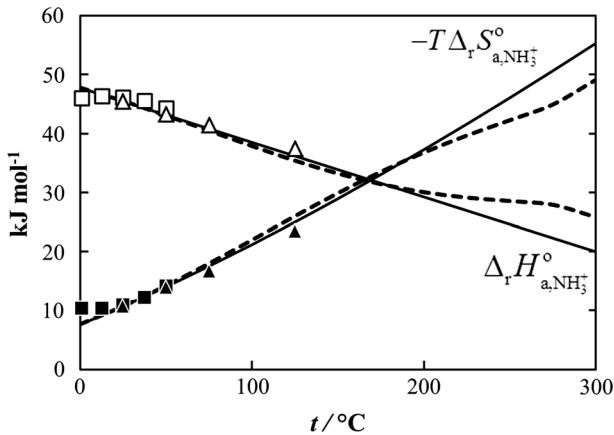


Fig. 11 Comparison between results for $\Delta_r H_{a,\text{NH}_3^+}^\circ$ and $-T\Delta_r S_{a,\text{NH}_3^+}^\circ$ for DL-2-aminobutyric acid obtained from the extended van't Hoff model and the predicted results from group additivity: *continuous lines*, calculated with Eq. 32 ($\Delta_r H_{a,\text{NH}_3^+}^\circ$) or Eq. 33 ($-T\Delta_r S_{a,\text{NH}_3^+}^\circ$); *dashed lines*, predicted with the group additivity model (Yezdimer et al. [11]). *Points* correspond to data from the literature. *Open points*: $\Delta_r H_{a,\text{NH}_3^+}^\circ$ and *solid points*: $-T\Delta_r S_{a,\text{NH}_3^+}^\circ$; *squares*, Smith et al. [16]; *triangles*, Gillespie et al. [23]

$1.0) \text{ J}\cdot\text{K}^{-1}\cdot\text{mol}^{-1}$ and $\Delta_r C_p^\circ_{a,\text{COOH}} = (-100.6 \pm 0.8) \text{ J}\cdot\text{K}^{-1}\cdot\text{mol}^{-1}$, respectively. The group additivity prediction also compares poorly with the average values for glycine $\Delta_r C_p^\circ_{a,\text{COOH}} = -187 \text{ J}\cdot\text{K}^{-1}\cdot\text{mol}^{-1}$ and 2-alanine $\Delta_r C_p^\circ_{a,\text{COOH}} = -141 \text{ J}\cdot\text{K}^{-1}\cdot\text{mol}^{-1}$ from Clarke et al. [25].

Results for the second ionization reaction are shown in Fig. 11. Again, the plots compare the predicted values for $\Delta_r H_{a,\text{NH}_3^+}^\circ$ and $-T\Delta_r S_{a,\text{NH}_3^+}^\circ$ with the experimental values

from this study and from the literature. In this case, the difference between the two trends is smaller and only happens at temperatures above 200 °C. For this reaction, the difference between the average value for $\Delta_r C_{p\text{ a, NH}_3^+}^{\circ}$ between (0 and 125) °C from the model ($-97.0 \text{ J}\cdot\text{K}^{-1}\cdot\text{mol}^{-1}$) agrees with the values obtained in this study from the extended van't Hoff model for DL-2-aminobutyric acid, $(-92.6 \pm 6.9) \text{ J}\cdot\text{K}^{-1}\cdot\text{mol}^{-1}$, and DL-norvaline, $(-110.3 \pm 6.7) \text{ J}\cdot\text{K}^{-1}\cdot\text{mol}^{-1}$, to within the experimental uncertainties. The value from the literature for 2-aminobutyric acid at 25 °C is $(-80 \pm 10) \text{ J}\cdot\text{K}^{-1}\cdot\text{mol}^{-1}$ [23].

The predictions for both ionization reactions show systematic deviations from the experimental results, large and positive for $pK_{\text{a, COOH}}$, small and negative for $pK_{\text{a, NH}_3^+}$. The magnitude of the deviations for the predicted values of $pK_{\text{a, COOH}}$ was unexpected. Although there are various possible causes for this behavior, there are two that we consider to be the most probable. The first is the calculated contributions for the charged groups. The limited number of available heat capacity data for the NH_3^+ group increases the uncertainty in the tabulated values for its contribution, as reported by Yezdimer et al. [11]. Deviations in the predicted values of $pK_{\text{a, NH}_3^+}$ are consistent with these uncertainties. The COO^- functional group contributions are thought to be more accurate because more data for standard partial molar volumes and heat capacities are available [11]. The deviations in extrapolated values of $pK_{\text{a, COOH}}$ are not consistent with these estimates. The second possible cause is that the functional groups, $\text{HOOC} - \overset{\text{O}}{\underset{\text{O}}{\text{C}}} - \text{NH}_3^+$ and $^- \text{OOC} - \overset{\text{O}}{\underset{\text{O}}{\text{C}}} - \text{NH}_2$, do not behave as simple combinations of the groups that form them due to interactions between the charged and uncharged polar entities. The results from this study suggest that this assumption is not valid for the first ionization reaction, and that the $-\text{NH}_3^+ - \text{COOH}$ interactions are so strong that they cannot be treated as independent groups on the same carbon atom. To test this finding, measurements of the standard molar heat capacities and volumes of the ionic forms of alkyl amino acids should be made over a wide range of temperature with the objective of measuring functional group contributions for the $\text{HOOC} - \overset{\text{O}}{\underset{\text{O}}{\text{C}}} - \text{NH}_3^+$ group and, possibly, the $^- \text{OOC} - \overset{\text{O}}{\underset{\text{O}}{\text{C}}} - \text{NH}_2$ group.

6 Conclusions

This is the first reported experimental study of the ionization constants of DL-2-aminobutyric acid and DL-norvaline at hydrothermal conditions, and the first for the second ionization constant of any amino acid above 125 °C. The results confirm the usefulness of UV–visible spectrophotometric flow cells with thermally stable colorimetric pH hydrothermal indicators as a means of measuring ionization constants at high pressures and temperatures with minimal effects from thermal decomposition of the sample. By writing both reactions in the isocoulombic form, the temperature dependent equilibrium constants could be fitted by a simple extended van't Hoff model, using constant values for $\Delta_r C_{p\text{ a}}^{\circ}$ as is expected for isocoulombic reactions. The values of $\Delta_r C_{p\text{ a, COOH}}^{\circ}$ and $\Delta_r C_{p\text{ a, NH}_3^+}^{\circ}$ obtained for both amino acids from the model are in good agreement with the limited data in the literature up to 125 °C. The values for the second ionization constant, $pK_{\text{a, NH}_3^+}$, at higher temperatures are consistent with extrapolations from the functional group additivity model reported by Yezdimer et al. [11] within the combined experimental and

model uncertainties. However, the extrapolated values of $pK_{a,COOH}$ are not consistent with the group additivity predictions. This finding suggests that the $-NH_3^+$ and $-COOH$ moieties cannot be treated as independent groups on the same carbon atom, and that it may be necessary to treat $HOOC - \overset{|}{\underset{|}{C}} - NH_3^+$ as a distinct functional group. More data for the thermodynamic properties of the ionized alkyl amino acid species at elevated temperatures are needed to test these findings and to improve the group additivity model's predictive abilities for amino acids under acidic and basic conditions.

We also note the need for improved experimental values for the thermally stable pH indicators used in this study. The values of $K_{a,COOH}$ obtained by using the ionization constant of acridine, K_{HAcr^+} , developed by Ryan et al. [26], showed an overall better agreement than the ones obtained from the expression by Minubayeva et al. [35]. Differences between our results for the same solution of 2-aminobutyric acid at 200 °C, using 2-naphthoic acid [28] and 4-nitrophenol [36] as indicators, required us to recalculate the ionization constants of 2-naphthoic acid reported by Xiang and Johnston [28]. Clearly, more calibration measurements are needed to reach the accuracy of which this important class of pH indicators are capable.

Acknowledgements This research was supported by the National Science and Engineering Research Council of Canada (NSERC), and by the “Apoyo a Doctorados Nacionales 2004” program from Colciencias, which provided a Ph.D. travel scholarship to D. E. Nieto Roca. We are grateful to Dr. Liliana Trevani and Dr. Jenny Cox who provided technical advice, scientific input and encouragement. We are also grateful to Mr. Ian Renaud and Mr. Case Gielen of the electronics shop and machine shop in the College of Physical and Engineering Science at the University of Guelph for their very considerable expertise in constructing and maintaining the UV–visible flow cell system. The functional group additivity calculations were carried out by Prof. Dr. Josef Sedlbauer at the University of Liberec in the Czech Republic, who also provided insightful advice and encouragement.

Appendix: Ionization Constant for 2-Naphthoic acid

As stated in the text, the temperature dependence of the ionization constant of 2-naphthoic acid was recalculated. Table 8 shows the results for the ionization constant of DL-2-aminobutyric acid at 200 °C obtained in this study with the two indicators. The value obtained with 4-nitrophenol was used as the true value for the constant at this temperature. The new ionization constant for 2-naphthoic acid was found by rearranging Eq. 21 to

$$K_{HIInd} = K_{a,NH_3^+} \frac{m_{HA^\pm}}{m_{A^-}} \cdot \frac{m_{Ind}}{m_{HIInd}} = \frac{K_{a,NH_3^+}}{\left(\frac{m_{A^-}}{m_{HA^\pm}}\right) \left(\frac{m_{HIInd}}{m_{Ind}}\right)} \quad (A1)$$

with the values of indicator and buffer ratios obtained for the spectra of 2-naphthoic acid at 200 °C. These results are listed in Table 12.

The extended van't Hoff model was used to establish the temperature dependence of $K_{2-NaphCOOH}$. As noted before, this model works well with isocoulombic reactions, where the assumption of small and constant $\Delta_r C_p^\circ$ is valid. For this reason, the reaction for the ionization of 2-naphthoic acid (Eq. 11) was rewritten as



where

Table 12 Experimental values of 2-naphthoic acid, $pK_{2-NaphCOOH}$, at $(200 \pm 0.1)^\circ\text{C}$

$pK_{a,NH_3^+}^a$	D^b	Buffer ratio ^c	Indicator ratio ^d	k	l	$pK_{2-NaphCOOH}^e$	Average ^g
						Experimental ^f	
7.1027 ± 0.0342	1.000	0.1045	0.06271	0.0591 ± 0.0015	0.9431 ± 0.0030	4.919 ± 0.013	4.359 ± 0.866
	1.004	0.1437	0.03433	0.0328 ± 0.0015	0.9547 ± 0.0029	4.796 ± 0.022	

^a Second ionization constant for DL-2-aminobutyric acid at $200.0 \pm 0.1^\circ\text{C}$ as determined with 4-nitrophenol as indicator

^b Defined as m_{acid}^*/m_{base}

^c Defined as $m_A/m_{HA^{\pm}}$

^d Defined as m_{HInd}/m_{Ind}

^e From Eq. A1

^f Uncertainty calculated from fitting parameters k and l

^g Uncertainty from standard deviation of average

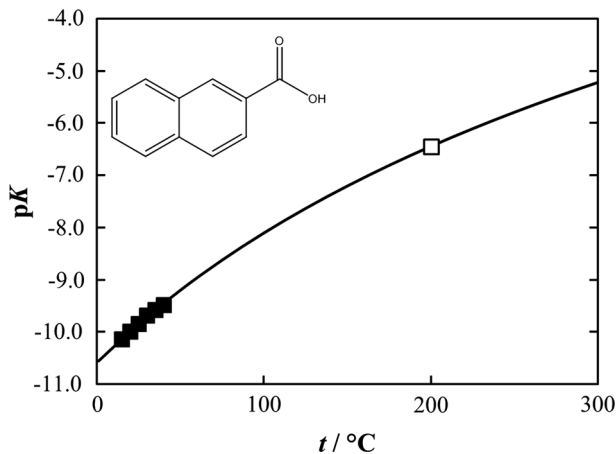


Fig. 12 Experimental values for the first ionization constant of 2-naphthoic acid, $pK_{\text{OH},2\text{-NaphCOOH}}$ (Eq. A2), plotted as a function of temperature. *Solid squares* correspond to data from literature (Briggs et al. [51]). *Open square* shows the result from this study

$$K_{\text{OH},2\text{-NaphCOOH}} = \frac{K_{2\text{-NaphCOOH}}}{K_{\text{w}}} = \frac{m_{\text{Ind}}}{m_{\text{HInd}} \cdot m_{\text{OH}^-}} \quad (\text{A3})$$

Results from literature for $K_{2\text{-NaphCOOH}}$ from Briggs et al. [51] and our result for 200 °C were used to calculate $K_{\text{OH},\text{NaphCOOH}}$, along with data for water from Sweeton et al. [41]. Equation 29 was then fitted to $K_{\text{OH},\text{NaphCOOH}}$, using $\Delta_{\text{r}}H_{\text{NaphCOOH}}^{\circ}$ and $\Delta_{\text{r}}H_{\text{w}}^{\circ}$ at 25 °C from the same sources, obtaining a value for $\Delta_{\text{r}}C_{\text{p}}^{\circ}$ of $-306.3 \pm 7.3 \text{ J}\cdot\text{mol}^{-1}\cdot\text{K}^{-1}$. The results from the fitting can be seen in Fig. 12.

References

1. Kharakoz, D.P.: Volumetric properties of proteins and their analogs in diluted water solutions. 1. Partial volumes of amino acids at 15–55 °C. *Biophys. Chem.* **34**, 115–125 (1989)
2. Lyon, S.: Materials science: a natural solution to corrosion? *Nature* **427**, 406–407 (2004)
3. Baross, J.A., Deming, J.W.: Growth of ‘black smoker’ bacteria at temperatures of at least 250 °C. *Nature* **303**, 423–426 (1983)
4. Crabtree, R.H.: Where smokers rule. *Science* **276**, 222 (1997)
5. Hamborg, E.S., Niederer, J.P.M., Versteeg, G.F.: Dissociation constants and thermodynamic properties of amino acids used in CO₂ absorption from (293 to 353) K. *J. Chem. Eng. Data* **52**, 2491–2502 (2007)
6. Yang, N., Xu, D.-Y., Wei, C.-C., Puxty, G., Yu, H., Maeder, M., Norman, S., Feron, P.: Protonation constants and thermodynamic properties of amino acid salts for CO₂ capture at high temperatures. *Ind. Eng. Chem. Res.* **53**, 12848–12855 (2014)
7. Cohn, E.J., Edsall, J.T.: *Proteins, Amino Acids, and Peptides as Ions and Dipolar Ions*. Hafner Publishing Company, New York (1943)
8. Romero, C.M., Negrete, F.: Effect of temperature on partial molar volumes and viscosities of aqueous solutions of alpha-DL-aminobutyric acid, DL-norvaline and DL-norleucine. *Phys. Chem. Liq.* **42**, 261–267 (2004)
9. Millero, F.J., Lo Surdo, A., Shin, C.: The apparent molal volumes and adiabatic compressibilities of aqueous amino acids at 25 °C. *J. Phys. Chem.* **82**, 784–792 (1978)
10. Amend, J.P., Helgeson, H.C.: Group additivity equations of state for calculating the standard molal thermodynamic properties of aqueous organic species at elevated temperatures and pressures. *Geochim. Cosmochim. Acta* **61**, 11–46 (1997)

11. Yezdimer, E.M., Sedlbauer, J., Wood, R.H.: Predictions of thermodynamic properties at infinite dilution of aqueous organic species at high temperature via functional group additivity. *Chem. Geol.* **164**, 259–280 (2000)
12. Tanger, J.C., Helgeson, H.C.: Calculation of the thermodynamic and transport properties of aqueous species at high pressures and temperatures; revised equations of state for the standard partial molal properties of ions and electrolytes. *Am. J. Sci.* **288**, 19–98 (1988)
13. Shock, E.L., Oelkers, E.H., Johnson, J.W., Sverjensky, D.A., Helgeson, H.C.: Calculation of the thermodynamic properties of aqueous species at high pressures and temperatures. Effective electrostatic radii, dissociation constants and standard partial molal properties to 1000 °C and 5 kbar. *J. Chem. Soc. Faraday Trans. I* **88**, 803–826 (1992)
14. Sedlbauer, J., O'connell, J.P., Wood, R.H.: A new equation of state for correlation and prediction of standard molal thermodynamic properties of aqueous species at high temperatures and pressures. *Chem. Geol.* **163**, 43–63 (2000)
15. Srivastava, J.P.N., Srivastava, M.N.: Stability constants and thermodynamic functions of some rare earth metal ion chelates of DL- α -aminobutyric acid. *J. Inorg. Nucl. Chem.* **40**, 2076–2078 (1978)
16. Smith, P.K., Taylor, A.C., Smith, E.R.B.: Thermodynamic properties of solutions of amino acids and related substances. III. The ionization of aliphatic amino acids in aqueous solution from one to fifty degrees. *J. Biol. Chem.* **122**, 109–123 (1937)
17. Israeli, M., Pettit, L.D.: Complex formation between unsaturated α -aminoacids and silver(I) and some divalent transition metal ions. *J. Inorg. Nucl. Chem.* **37**, 999–1003 (1975)
18. Gergely, A., Sóvágó, I.: Log β , ΔH and ΔS values of mixed complexes of Cu(II) with histamine and some aliphatic aminoacids. *J. Inorg. Nucl. Chem.* **35**, 4355–4365 (1973)
19. Gergely, A., Sóvágó, I., Nagypaál, I., Király, R.: Equilibrium relations of alpha-aminoacid mixed complexes of transition metal ions. *Inorg. Chim. Acta* **6**, 435–439 (1972)
20. Datta, S.P., Grzybowski, A.K.: The second acid dissociations of glycine, sarcosine and N-dimethylglycine. Part 1. -Thermodynamic dissociation constants. *Trans. Faraday Soc.* **54**, 1179–1187 (1958)
21. Datta, S.P., Grzybowski, A.K.: The second acid dissociations of glycine, sarcosine and N-dimethylglycine. Part 2. -Thermodynamic quantities. *Trans. Faraday Soc.* **54**, 1188–1194 (1958)
22. Anderson, K.P., Newell, D.A., Izatt, R.M.: Formation constant, enthalpy, and entropy values for the association of alanine with H and Cu_2^+ at 10, 25, and 40 °. *Inorg. Chem.* **5**, 62–65 (1966)
23. Gillespie, S.E., Oscarson, J.L., Izatt, R.M., Wang, P., Renuncio, J.A.R., Pando, C.: Thermodynamic quantities for the protonation of amino acid amino groups from 323.15 to 398.15 K. *J. Solution Chem.* **24**, 1219–1247 (1995)
24. Wang, P., Oscarson, J.L., Gillespie, S.E., Izatt, R.M., Cao, H.: Thermodynamics of protonation of amino acid carboxylate groups from 50 to 125 °C. *J. Solution Chem.* **25**, 243–266 (1996)
25. Clarke, R.G., Collins, C.M., Roberts, J.C., Trevani, L.N., Bartholomew, R.J., Tremaine, P.R.: Ionization constants of aqueous amino acids at temperatures up to 250 °C using hydrothermal pH indicators and UV-visible spectroscopy: glycine, alpha-alanine, and proline. *Geochim. Cosmochim. Acta* **69**, 3029–3043 (2005)
26. Ryan, E.T., Xiang, T., Johnston, K.P., Fox, M.A.: Absorption and fluorescence studies of acridine in subcritical and supercritical water. *J. Phys. Chem. A* **101**, 1827–1835 (1997)
27. Xiang, T., Johnston, K.P.: Acid–base behavior of organic compounds in supercritical water. *J. Phys. Chem.* **98**, 7915–7922 (1994)
28. Xiang, T., Johnston, K.P.: Acid–base behavior in supercritical water: β -Naphthoic acid-ammonia equilibrium. *J. Solution Chem.* **26**, 13–30 (1997)
29. Hakin, A.W., Daisley, D.C., Delgado, L., Liu, J.L., Marriott, R.A., Marty, J.L., Tompkins, G.: Volumetric properties of glycine in water at elevated temperatures and pressures measured with a new optically driven vibrating-tube densimeter. *J. Chem. Thermodyn.* **30**, 583–606 (1998)
30. Clarke, R.G., Tremaine, P.R.: Amino acids under hydrothermal conditions: apparent molar volumes of α -alanine, β -alanine and proline at temperatures from 298 to 523 K and pressures up to 20.0 MPa. *J. Phys. Chem. B* **103**, 5131–5144 (1999)
31. Clarke, R.G., Hnedkovský, L., Tremaine, P.R., Majer, V.: Amino acids under hydrothermal conditions: apparent molar heat capacities of aqueous β -Alanine, β -alanine, glycine, and proline at temperatures from 298 to 500 K and pressures up to 30.0 MPa. *J. Phys. Chem. B* **104**, 11781–11793 (2000)
32. Bulemela, E., Tremaine, P.R.: Standard partial molar volumes of some aqueous alkanolamines and alkoxyamines at temperatures up to 325 °C: functional group additivity in polar organic solutes under hydrothermal conditions. *J. Phys. Chem. B* **112**, 5626–5645 (2008)
33. Bulemela, E., Tremaine, P.R.: D2O isotope effects on the ionization constant of b-naphthol and boric acid at temperatures from 225 to 300 °C using UV-visible spectroscopy. *J. Solution Chem.* **38**, 805–826 (2009)

34. Trevani, L.N., Roberts, J.C., Tremaine, P.R.: Copper(II)–ammonia complexation equilibria in aqueous solutions at temperatures from 30 to 250 °C by visible spectroscopy. *J. Solution Chem.* **30**, 585–622 (2001)
35. Minubayeva, Z., Suleimenov, O.M., Seward, T.M.: Acridinium ion ionization at elevated temperatures and pressures to 200 °C and 2000 bar. *J. Solution Chem.* **37**, 291–305 (2008)
36. Ehlerova, J., Trevani, L.N., Sedlbauer, J., Tremaine, P.R.: Spectrophotometric determination of the ionization constants of aqueous nitrophenols at temperatures up to 225 °C. *J. Solution Chem.* **37**, 857–874 (2008)
37. Holmes, H.F., Mesmer, R.E.: Isopiestic studies of aqueous solutions at elevated temperatures VII. MgSO₄ and NiSO₄. *J. Chem. Thermodyn.* **15**, 709–719 (1983)
38. Christensen, J.J., Oscarson, J.L., Izatt, R.M.: Thermodynamics of proton ionization in dilute aqueous solution. X. ΔG° (pK), ΔH° , and ΔS° values for proton ionization from several monosubstituted carboxylic acids at 10, 25, and 40°. *J. Am. Chem. Soc.* **90**, 5949–5953 (1968)
39. Anderson, G.M., Crerar, D.A.: *Thermodynamics in Geochemistry: The Equilibrium Model*. Oxford University Press, New York (1993)
40. Mesmer, R.E., Marshall, W.L., Palmer, D.A., Simonson, J.M., Holmes, H.F.: Thermodynamics of aqueous association and ionization reactions at high-temperatures and pressures. *J. Solution Chem.* **17**, 699–718 (1988)
41. Sweeton, F.H., Mesmer, R.E., Baes Jr., C.F.: Acidity measurements at elevated temperatures. VII. Dissociation of water. *J. Solution Chem.* **3**, 191–214 (1974)
42. Kay, R.L.: The current state of our understanding of ionic mobilities. *Pure Appl. Chem.* **63**, TBD, 1393–1399 (1991)
43. Tremaine, P., Arcis, H.: Solution calorimetry under hydrothermal conditions. *Rev. Mineral. Geochem.* **76**, 219–263 (2013)
44. Fawcett, W.R.: Liquids, solutions, and interfaces: In: *Classical Macroscopic Descriptions to Modern Microscopic Details*. Oxford University Press, New York (2004)
45. Tremaine, P.R., Zhang, K., Bénézech, P., Xiao, C.: In: Palmer, D.A., Fernandez-Prini, R., Harvey, A.H. (eds.) *Aqueous Systems at Elevated Temperatures and Pressures: Physical Chemistry in Water, Steam and Aqueous Solutions*, Chap. 13. Academic Press, Amsterdam (2004)
46. Hakin, A.W., Duke, M.M., Klassen, S.A., McKay, R.M., Preuss, K.E.: Apparent molar heat capacities and volumes of some aqueous solutions of aliphatic amino acids at 288.15, 298.15, 313.15, 328.15 K. *Can. J. Chem.* **72**, 362–368 (1994)
47. Domalski, E.S.: Heats of combustion and formation of organic compounds containing the elements C, H, N, O, P and S. *J. Phys. Chem. Ref. Data* **1**, 221–277 (1972)
48. Hakin, A.W., Liu, J.L.: The calorimetric and volumetric properties of selected α -amino acids and α , ω -amino acids in water at T = (288.15, 298.15, 313.15, and 328.15) K and p = 0.1 MPa. *J. Solution Chem.* **35**, 1157–1171 (2006)
49. Huffman, H.M., Fox, S.W., Ellis, E.L.: Thermal data. VII. The heats of combustion of seven amino acids. *J. Am. Chem. Soc.* **59**, 2144–2150 (1937)
50. Huffman, H.M., Ellis, E.L., Fox, S.W.: Thermal data. VI. The heats of combustion and free energies of seven organic compounds containing nitrogen. *J. Am. Chem. Soc.* **58**, 1728–1733 (1936)
51. Briggs, A.G., Tickle, P., Wilson, J.M.: Acid–base equilibria of some naphthoic acids, studied spectrophotometrically. *Spectrochim. Acta, Part A* **26**, 1399–1402 (1970)